5-2008

Experimental Measurement of Thermal Conductivity of an Unknown Material

Aaron Christopher Whaley
University of Tennessee - Knoxville

To the Graduate Council:

I am submitting herewith a thesis written by Aaron Christopher Whaley entitled "Experimental Measurement of Thermal Conductivity of an Unknown Material." I have examined the final electronic copy of this thesis for form and content and recommend that it be accepted in partial fulfillment of the requirements for the degree of Master of Science, with a major in Mechanical Engineering.

Rao V. Arimilli, Major Professor

We have read this thesis and recommend its acceptance:

Majid Keyhani, Jay I. Frankel

Accepted for the Council:
Dixie L. Thompson

Vice Provost and Dean of the Graduate School

(Original signatures are on file with official student records.)

To the Graduate Council:

I am submitting herewith a thesis written by Aaron Christopher Whaley entitled "Experimental Measurement of Thermal Conductivity of an Unknown Material." I have examined the final electronic copy of this thesis for form and content and recommend that it be accepted in partial fulfillment of the requirements for the degree of Master of Science, with a major in Mechanical Engineering.

Rao V. Arimilli, Major Professor

_____

We have read this thesis and recommend its acceptance:

Majid Keyhani

_____

Jay I. Frankel

_____

Accepted for the Council:

Carolyn R. Hodges, Vice Provost
and Dean of the Graduate School

_____

(Original signatures are on file with official student records.)

Experimental Measurement of Thermal Conductivity of an Unknown Material

A Thesis Presented for
The Master of Science
Degree
The University of Tennessee, Knoxville

Aaron Christopher Whaley
May 2008

Acknowledgments

I wish to thank everyone involved in helping me to complete my Masters of Science in Mechanical Engineering. I would like to thank Dr. Arimilli for his guidance through the design of the research project. I thank Dr. Keyhani for his valuable input to the research project. I also thank Dr. Arimilli and Dr. Keyhani for their teaching and experience, which improved my understanding of engineering. I thank Dr. Frankel for serving on my committee. I also would like to thank PhD student Kirk Lowe for leading the experiment, assisting in my comprehension of the measurement process, and providing various forms of advice.

Last, but not least, I thank God, my family, and my friends for getting me where I am today.

Abstract

The objective of this study was to determine effective thermal conductivity of an unknown material sample for sample temperatures up to 1000 degrees Celsius. A steady state, one-dimensional heat conduction test setup was designed, fabricated, assembled, and used to determine thermal conductivity of the sample. The measurement was accomplished by applying a heat flux from a radiant heater through a stack consisting of the test sample, reference plates, heat spreaders, and insulation layers. The heat transfer equation for steady state, one-dimensional conduction relates thermal conductivity of the sample to the thickness and cross-sectional area of the sample, the temperature difference across the sample, and the one-dimensional heat transfer rate through the sample. Thus, the thermal conductivity was calculated and assigned to the mean temperature of the sample for each particular run. One-dimensional heat transfer was maintained by guard heaters and insulation placed around the stack to reduce heat losses to the surroundings. Heat transfer through the sample was determined by subtracting the heat losses from the main power supply. A novel feature of the final-design configuration utilizes a "cold side" heater at the cold end of the stack to elevate the temperature within the stack without significantly increasing the power supply to the main heater. The experimental thermal conductivity results ranged from 4.90 to 9.93 W/(m K) over a temperature range between 208 and 865 degrees Celsius. A correlation for thermal conductivity over the temperature range is presented. With an uncertainty analysis of the thermal conductivity results, it was shown that the average calculated uncertainty was 3% of the final results.

Table of Contents

List of Figures

List of Symbols

q	heat transfer rate through the sample (W)
k	thermal conductivity of the sample (W/(m K))
A	area of the sample perpendicular to the heat flow direction (m^2)
ΔT	temperature difference across the sample (K)
Δx	thickness of the sample through which 1-D heat flows (m)
ω	uncertainty (± unit of interest)
δ	penetration depth (m)
c	constant (Equation 3)
α	thermal diffusivity of material (m^2/s)
t	time (s)
ρ	density (kg/m^3)
C_P	specific heat (J/(kgK))
q_{stack}	one-dimensional heat transfer through stack (W)
$q_{Main\ Heater}$	main heater power supply (W)
q_{loss}	heat loss in lateral or back of main heater direction (W)
∂	partial derivative operator
$\sum$	summation operator
q_{R1}	heat transfer rate through reference plate 1 (W)
q_{R2}	heat transfer rate through reference plate 2 (W)
SS	stainless steel (subscript)
SiC	silicon carbide

Chapter 1. Introduction

In nearly all engineering applications, an important consideration is the choice of material. It is vital to understand the various properties of a material that will determine how that material will react or respond to a given situation. Physical properties of particular interest are thermophysical properties, which define characteristics of heat transport and heat storage in a material. Knowledge of the properties depends on adequate data produced from experiment. The scope of this work focuses on the measurement of one thermophysical property, namely the thermal conductivity.

The thermal conductivity of a material indicates the ability of the material to transport heat energy [1]. Heat energy is transported through a material by several means, including electrons, lattice waves (or phonons), electromagnetic waves, and many others [1]. Metals transport heat primarily through the motion of electrons, while nonmetals essentially transport heat in the form of wave packets propagating through the lattice structure of the material [1]. Thermal conductivity is not a constant property, as it varies primarily with temperature for isotropic materials. For any particular material, thermal conductivity is reported as a function of temperature. The composition of the material determines the specific behavior of thermal conductivity versus temperature. Most materials used for thermal conductivity measurements are nonmetals that have more complex structures, and therefore more intriguing results. The ability to conduct heat is either aided or hindered by the type of structure, since the conduction of heat in a nonmetal is a wave traveling through the lattice structure of atoms and molecules [1]. Conduction of heat is aided by uniform, organized structures of atoms and molecules.

Conduction is hindered by obstructions that clutter the structure and disrupt the natural flow of heat. Material "clutter", such as grain boundaries, lattice defects, dislocations, and various imperfections present in a material will deter the transport of heat, thus producing a low value of thermal conductivity. On the other hand, the fewer the obstacles, the easier it is for the material to conduct heat, and the thermal conductivity will be high. The previously mentioned obstacles that oppose heat flow are only a few of the many factors that influence thermal conductivity, making the measurement and understanding of this property of much complexity and interest.

The measurement of thermal conductivity is not a direct or exact procedure. The task of determining the thermal conductivity (k) of an unknown material generally involves the use of heat transfer equations and theory. There are several methods of experimentally determining thermal conductivity, such as the steady state or comparative method, the radial flow method, the laser-flash diffusivity method, and the pulse-power method [1]. The major contributor of the work stems from the design and recorded results of one experimental method, while the background information on thermal conductivity measurement supplements the understanding of the process. The specific method of measuring thermal conductivity being considered is the application of one-dimensional, steady state conduction heat transfer, namely the comparative method. The experiment will force this type of heat transfer such that thermal conductivity values can be generated through the relevant heat transfer equation.

The objective of the experiment is to determine thermal conductivity for an unknown material sample over a range of sample temperatures, thus generating a possible function, k(T). The material supplied for testing is a nonmetal, best described as a

composite consisting of silicon carbide. This experiment is unique in that it is to be conducted at high temperatures (up to 1000°C). Achieving such temperatures requires much attention on design and safety. The work provides a setup for measuring any unknown material under similar conditions, while at the same time revealing the uncertainties in the final results.

Chapter 2. Literature Review

A literature review of two sources was conducted. The purpose of the chosen sources was to explore the methods of testing of thermal conductivity, specifically the steady state comparative method. The literature is listed in the References section.

2.1: Background Review on Measurement Procedures

Several thermal conductivity measurement techniques exist, and the proper technique depends on many factors, such as sample type, temperature range, and available resources. The common denominator of all the techniques is that accuracy is difficult to achieve and is by no means a routine challenge.

The simplest design is the steady state method [1]. The test sample is sandwiched between a heat source and a heat sink, allowing a temperature gradient to exist across the sample. After steady state is reached, the measured temperature difference across the sample (provided by thermocouples), the physical dimensions of the sample, and the estimated heat flow through the sample produce the thermal conductivity by applying Fourier's law for one-dimensional steady state heat conduction (Equation 1).

$$q = kA\frac{\Delta T}{\Delta x} \qquad (1)$$

Essential to the calculation of thermal conductivity are the stack heat flow (q), the temperature difference across the sample (ΔT), and the physical dimensions of the sample (thickness, Δx, and cross-sectional area, A). The basic application of Equation 1 is shown in a schematic in Figure 2.1.

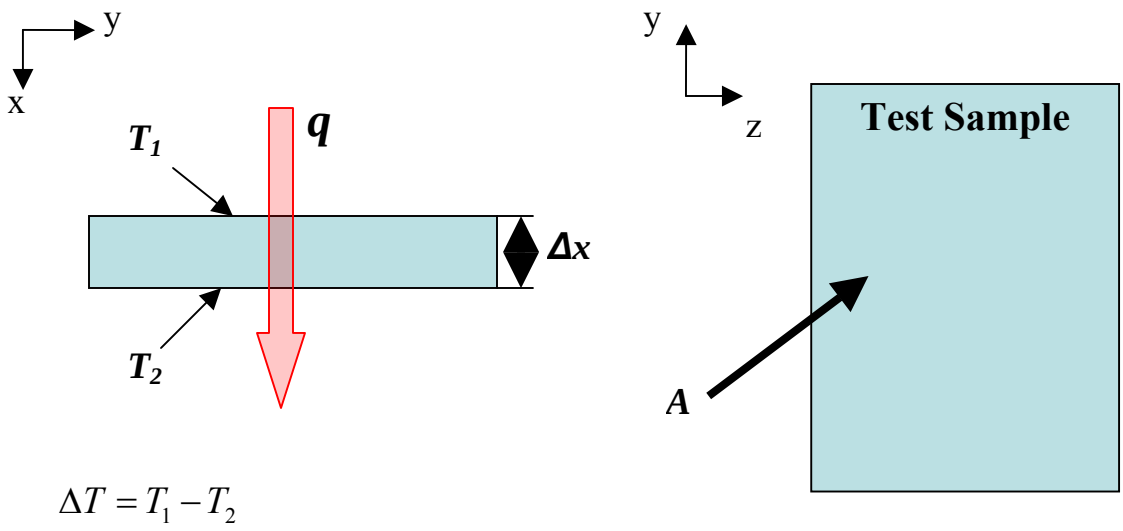

Figure 2.1: Schematic of steady state conduction through a test sample

The one-dimensional, steady state conduction equation involves heat flux, temperature change, physical dimensions of the heat transfer system, and thermal conductivity. With the knowledge of the physical dimensions of the sample, as well as temperatures and heat supplied, the thermal conductivity can be calculated. The accuracy of such a measurement procedure depends greatly on the estimation of one-dimensional heat supply. The amount of heat delivered may be known, but one must account for and subtract any heat losses due to thermal radiation, convection currents, or conduction in any direction other than the specified heat flow direction. Heat loss can not be fully prevented, but must be minimized with careful design. For instance, good thermal contact must exist around the sample to reduce air gaps. Insulation and heat shields are helpful to reduce lateral conduction and thermal radiation loss, respectively. The advantage of this method is the simplicity of assembly; however, the disadvantage is that thermal radiation loss to the surroundings becomes significant at high temperatures. The

experiment can be performed at high temperatures, but accounting for and reducing thermal radiation becomes more difficult.

The comparative method takes the idea of the steady state method and adds a reference material (sandwiched between the source and sink, next to test sample) with known properties to compare with the unknown specimen. Equation 1 still applies, and the comparison of the temperature behavior of the reference material to the temperature behavior of the test sample provides a more certain measurement of thermal conductivity. Though the added component to the stack increases the sources of heat loss to account for, the accuracy of the measurement depends more strongly on the certainty of the reference material properties. This was the chosen technique for the conducted experiment, and will be explained in further detail by a review of the ASTM book of standards [2].

Other more complex methods are also available to measure thermal conductivity, including the radial flow method, the laser-flash diffusivity method, and the pulse-power method [1]. Due to limited resource availability, as well as the understanding of the possible applications of the rectangular samples that were supplied for testing, the comparative method was the most suitable choice.

The radial flow method involves circular or cylindrical geometry with an internal heat source [1]. This method greatly minimizes the thermal radiation loss radially, since the supplied heat flow is also radial. The conduction equation in the appropriate coordinate system (cylindrical, for example) generates the thermal conductivity with all temperatures, heat flows, and physical dimensions known. The drawback to this method is that it requires rather large sample sizes which may not be feasible to obtain for research materials.

The laser-flash diffusivity method calculates the thermal diffusivity of a material. One face of a sample is irradiated by a short laser pulse, and the temperature response of the opposite face is recorded [1]. The temperature rise versus time profile is used to calculate thermal diffusivity, and if the density and specific heat are known, thermal conductivity can be calculated. The advantage of this method is the short test time, as waiting for steady state is not an issue. However, the sample requirements can be strict, since the sample surfaces must have a high absorptivity.

The pulse-power method (or Maldonado technique) uses a current pulse supplied to a heater through a sample [1]. This is another transient method, not requiring steady state. This method is commercially used because of its accuracy. The parallel thermal conductance technique is intended for small samples, while the Harman technique is used for thermoelectric materials. All of these methods can be explored further if there is any particular interest, but the concentration of this work will be the use of the comparative method.

2.2: Literature Review of Comparative Method

The ASTM standards book series provides test methods for determining thermal conductivity experimentally. The procedure described for testing materials at high temperatures is known as the guarded-comparative-longitudinal heat flow technique [2]. This method for determining thermal conductivity (k) for various homogeneous, opaque solids is a steady state technique, utilizing one-dimensional heat conduction equations. The test method is specified to be used for a thermal conductivity range of 0.2 – 200 W/(m K), and a temperature range of 90 – 1300 Kelvin [2]. Generally, the test procedure

involves the specimen with unknown thermal conductivity placed under a load between two similar materials of known thermal properties, known as reference materials. The reference materials and specimen in contact form a longitudinal stack to which a temperature gradient is to be supplied from a heat source at one end, to a heat sink at the other end. Insulation and guarding are placed around the stack in order to minimize heat loss to the surroundings and essentially force the process to one-dimensional heat flow. Thermocouples are placed on either end of each material (specimen and two reference materials on either side) with careful consideration as to the acceptable distance between adjacent thermocouples to avoid interference [2]. After equilibrium of heat transfer is reached, the measured temperature gradients across the three instrumented components, the known thermal conductivity of the reference materials, the estimated amount of one-dimensional heat flow through the stack, and the known physical dimensions of the components are used to calculate the unknown thermal conductivity of the specimen. The heat conduction equations for one-dimensional steady state flow relate the known values to the unknown thermal conductivity.

2.2.1: Reference Materials

The reference materials' properties, namely thermal conductivity, should be as close as possible to the unknown specimen properties, and must demonstrate stability over the temperature range [2]. The reason for the desired similarity between the reference material and the specimen arises from the fact that heat shunting errors may occur during the process when the adjacent materials have drastically different thermal conductivities [2]. In other words, the direction of the flow of heat may be significantly altered when transferring from the reference to the specimen (or vice versa) if there is a

large difference in thermal conductivity between the two materials. Also, when deciding between two possible reference materials, the material with the higher thermal conductivity should be used to further aid the overall heat flow [2]. Since there is essentially nothing known about the specimen, educated estimations based on the general composition of the specimen should produce an adequate reference material. The purpose of the reference material is to provide a means of acquiring the amount of heat flowing one-dimensionally through the stack. The accuracy of that measurement depends more on how well known the thermal conductivity of the reference material is, rather than how similar the material is to the specimen.

2.2.2: Insulation and Guarding

Insulation materials obtained should be easy to handle and must be usable over the desired temperature range. Insulation materials designed for high temperatures (as will be achieved in the experiment) reduce conduction due to the material composition and the presence of air gaps throughout the insulation. These materials also can reduce thermal radiation, which becomes more significant at high temperatures. High temperature fiber blankets are an acceptable choice, since they do not conduct electricity and are easily constructible to suit any particular need. Guarding includes heaters placed around the stack that will supply a small amount of heat (relative to the longitudinal stack heater) to greatly reduce the lateral heat loss. Insulation alone is not feasible at high temperatures since the amount of heat loss would require such a large amount of insulation that it would be extremely impractical to consider. The ideal guarding either has the same linear temperature gradient as the stack or a constant temperature equal to the average temperature of the stack [2]. This exact guarding will prevent lateral heat

flow. However, the complications involved in achieving exact guarding call for practical measures that will significantly reduce lateral heat flow, instead of fully preventing it.

The accuracy of the unknown thermal conductivity depends on the accuracy of the measured temperatures and the calculated one-dimensional heat flow. Therefore, it is important that there is appropriate insulation and guarding around the stack and minimization of contact resistance at the material interfaces, i.e. smooth surfaces, etc., to best approximate one-dimensional, uniform heat flow. The cross-sectional areas of the materials must also be as close to equal as possible to avoid error. The ASTM literature states that the design of the system is difficult and therefore not practical for a wide range of uses due to the amount of restrictions placed on the system. Conditions that lead to error include non-uniform heat transfer across interfaces, heat loss to surroundings, and heat shunting. This comparative method is most useful for engineering materials such as ceramics, polymers, and refractories, given that careful consideration is taken as well as the participants having adequate knowledge of the possible uncertainties involved.

Chapter 3. Design of Experimental Setup

For the experimental determination of thermal conductivity of the given silicon carbide sample over a range of temperatures up to 1000°C, the comparative method utilizing one-dimensional heat conduction was employed. The apparatus consisted of a stack of rectangular plates, including the test sample, reference materials, heat spreaders, and insulation. Radiant heaters were used to supply the heat flux and guarding to the stack. The details of the design progressively changed as certain issues required adjustments to test over the desired temperature range with as much accuracy as possible. The designs are labeled as configurations, and a description of the chronological order of design changes in addition to a display of the results obtained from each configuration are provided in Appendix A.

3.1: Objective of Design

The appropriate combination of stack components, insulation, guarding, and heater supply is needed to generate the desired range of sample temperatures. The designated sample temperature is an average of the temperatures on opposite sides of the sample. Therefore, the range of temperature drop across the sample must be carefully considered. If the temperature drop is small, the uncertainty of the temperature recordings from the thermocouples could overlap the actual temperature drop. If, for example, the thermocouple readings across the sample are 180ºC and 178 ºC, it is possible that the actual temperatures are 179 ºC and 181ºC, if the uncertainty of the thermocouples is high enough. In that case, the heat would actually be flowing in the opposite direction than the thermocouple readings would indicate. Also, if the

uncertainty is a significant percentage of the temperature drop, there is very little confidence in the accuracy of the temperature drop and, consequently, the thermal conductivity result. On the other hand, the temperature drop across the sample can not be too large. If the temperatures across the sample are 200 ºC and 150 ºC, the designated sample mean temperature is more inaccurate. Assigning a mean temperature of 175 ºC to such a broad temperature range in this case would be much more doubtful than if the temperatures are 180 ºC and 170 ºC, respectively. This precaution prevents the designer from simply supplying enormous amounts of power to the heater to achieve high temperatures, since the resultant sample temperature drop (ΔT in Equation 1) would continue to increase. Thus, adding thermal resistance to the stack is necessary to increase the total mean temperature of the stack. This approach does not require an increase in supplied power. With the same amount of heat supplied, the higher resistance created by the variable insulation results in a higher temperature difference between the heat source and the heat sink, and thus a higher mean temperature of the test sample. A consequence of this approach is that the time for the system to reach steady state increases as the total thermal resistance and capacitance of the stack increases. To efficiently and accurately achieve the desired sequence of test runs over the temperature range, the heat supply to the main heater and to the guard heaters should be balanced and integrated with appropriate thermal resistances.

3.2: Initial Design, Configuration A

The first implemented design had a heat source on top, with a heat sink underneath the stack. An isothermal chill plate served as the heat sink. This was

designated as configuration A. The isothermal plate consisted of two pieces of copper sandwiched together with internal grooves for internal water circulation. The water was cycled through the plate by a constant temperature bath regulator. A schematic of the stack is shown in Figure 3.1. The insulation around the stack reduced the heat flow escaping in the lateral direction, originating from the main heater. Guard heaters were in place to supply heat to the stack in the lateral direction in order to restrict most of the flow (~90-95%) to one dimension, i.e., through the stack. Stainless steel reference plates on both sides of the test sample contained six thermocouples each (3 on each surface), which allowed for monitoring of uniform temperature distribution at each surface of each plate, calculation of mean temperature of the sample, and calculation of heat flux through the stack. The thermocouples located in the insulation above the stack and around the stack (differential thermocouples) monitored the heat loss through the back of the main heater and the lateral heat loss, respectively. Another heater placed above the main heater was used to limit heat loss through the back of the main heater. In order to increase the mean temperature through the specified range, insulation layers would be placed between the aluminum plate and the stainless steel sheet. The power supply to the main heater was also increased in small amounts (~10-50W per step). The stainless steel sheet was in place so that the stack could be lifted in one piece as more variable insulation was added. The components of the stack, the guard heaters, and the surrounding insulation were held together by clamping tools, which maintained good thermal contact throughout the stack and reduced the amount of air gaps.

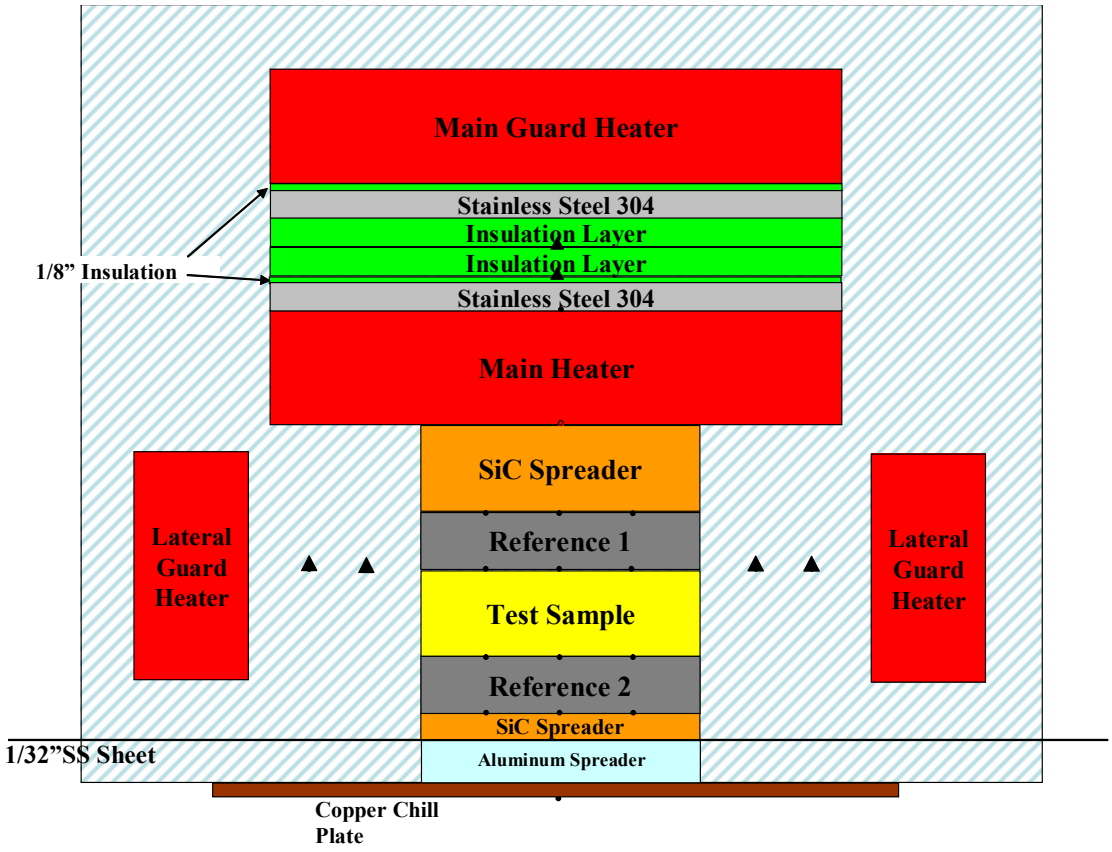

- thermocouple probe

▲ thermocouples across insulation

insulation

Figure 3.1: Configuration A, the initial schematic with the thin sample between reference plates

The surface finishes of the reference plates and the samples, especially, were not perfectly smooth in spite of repeated polishing with fine grit sand paper. Consequently, the small air gaps that existed between the plates represented thermal contact resistances hindering heat flow, even when the stack was compressed by applied weights. A procedure to eliminate the contact resistance between the sample and reference is to run a test for two different sample thicknesses. Two sample thicknesses that were provided were about 21/32" thick and 49/32" thick. The calculated difference between the total thermal resistance across the two reference plates and the test sample for both samples cancels out the contact resistance, assuming that the contact resistance is the same in the tests of both thicknesses. This procedure is useful for homogeneous solids, since the thermal conductivity of either sample thickness should be the same. However, for non-homogeneous solids, the change in thickness can greatly affect the resultant thermal conductivity measurement due to the additional random clutter present in the larger sample. Testing two thicknesses separately helps determine the degree of inhomogeneity present in the provided samples. Configuration A was adequate for low temperatures (<500ºC). For tests at higher temperatures, too much heat was lost through the stainless steel sheet at the bottom due to its size and the tendency for air gaps to form between it and the stack. Therefore, adjustments to the design were needed to address these issues.

3.3: Design Modifications for High Temperature Measurement, Configuration B

To achieve higher temperatures of the test sample without losing large amounts of heat to the surroundings, modifications to the guarding and stack design were required. Since the stainless steel plate was more of a hindrance than a help at elevated

temperatures, it was removed. In order to still be able to add insulation to the "cold" end of the stack easily, the stack was turned upside down, with the heat sink on top, and the heat source (main heater) on the bottom. A schematic of the design is shown in Figure 3.2. This design was designated as configuration B. Extra guard heaters were added around the entire perimeter of the stack such that there were two heaters in parallel on each of the four lateral sides. This addition limited lateral heat loss through corners and maintained more uniform guarding through the stack length. At the top of the stack, the heat sink was the copper chill plate with variable insulation beneath the plate. The variable insulation could be easily added to or removed from the stack with very minimal down time. The experiment was run starting at low temperatures for the thin, 21/32" sample. The constant temperature bath circulated cold water (~25 ºC) through the copper chill plate. This in turn required very high heater power input to the main heater to achieve sample temperatures greater than 500ºC. Added insulation alone was not enough to raise the stack temperature, and the increased power supply would increase heat loss to the surroundings, making the situation worse. Using the chill plate in tests of these higher temperatures simply would not be possible without seriously affecting the accuracy of the results. Therefore, the copper chill plate was removed for higher temperature measurements. It was replaced with another heater to produce even higher temperatures in the stack. This heater served as a specified "cold side" boundary condition. This heater supplied a small amount of power relative to the main heater, so as to serve as a heat sink. A combination of main heater supply, variable insulation, and cold side heater supply generated the higher sample temperatures.

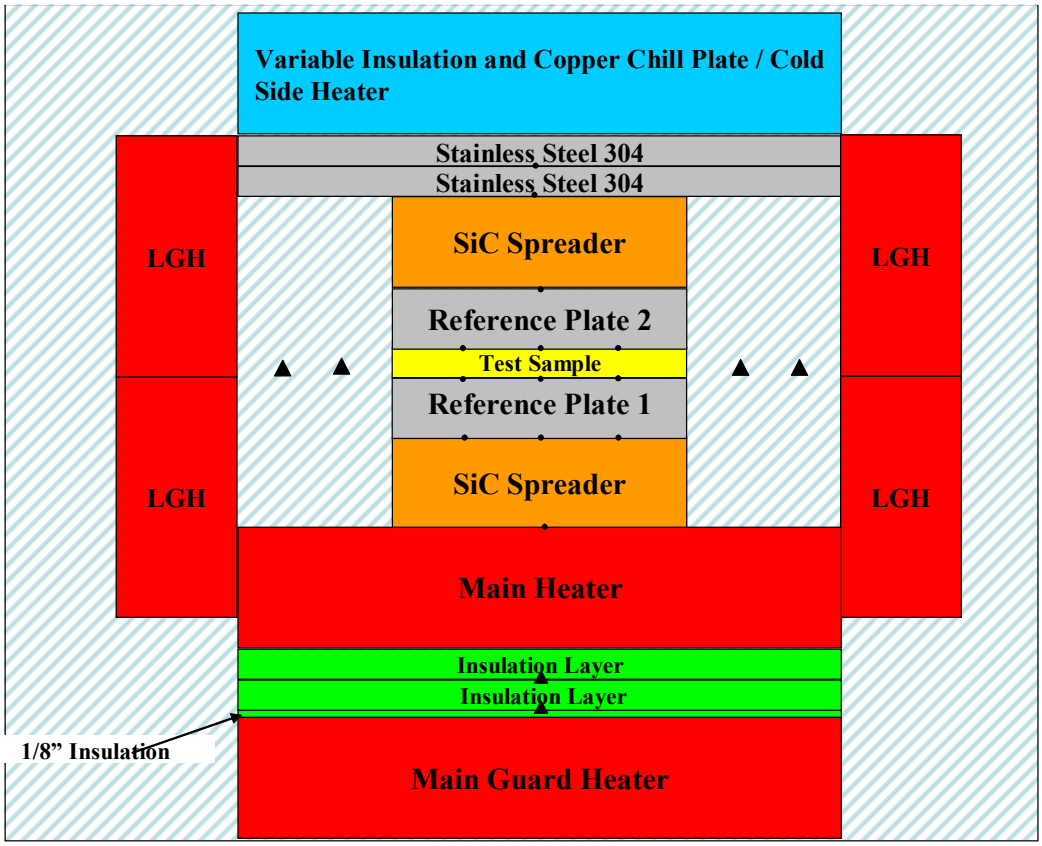

Figure 3.2: Configuration B schematic for high temperatures

Chapter 4. Test Procedure and Data Reduction

The system was considered to have reached steady state when the temperatures of the thermocouples throughout the stack reached steady values over time. A power supply (AC or DC) with several outlets controlled individually by knobs delivered the desired wattage to any of the utilized heaters. During each test run, the thermocouple readings from about 26 locations were sent to the appropriate number of channels of a data acquisition device. The data acquisition device cycled through all channels continuously. The recorded voltages were converted to temperature values and logged using an HP VEE program. The program plotted temperature versus time at the various thermocouple locations to monitor for steady state, lateral heat loss, and any other item of interest. A schematic of the equipment setup is shown in Figure 4.1. The reference voltage for the thermocouples was a constant value hardwired into the program originating from average data taken from an ice bath. Since each run took a day or more to reach steady state, maintaining an ice bath throughout the test was not very feasible. Hardwiring a constant reference may have slightly affected the accuracy of the mean temperature readings, but the emphasis of calculating a thermal conductivity value was on the accuracy of the temperature difference, not the accuracy of the temperature itself. The resultant thermal conductivity was at the approximate mean sample temperature.

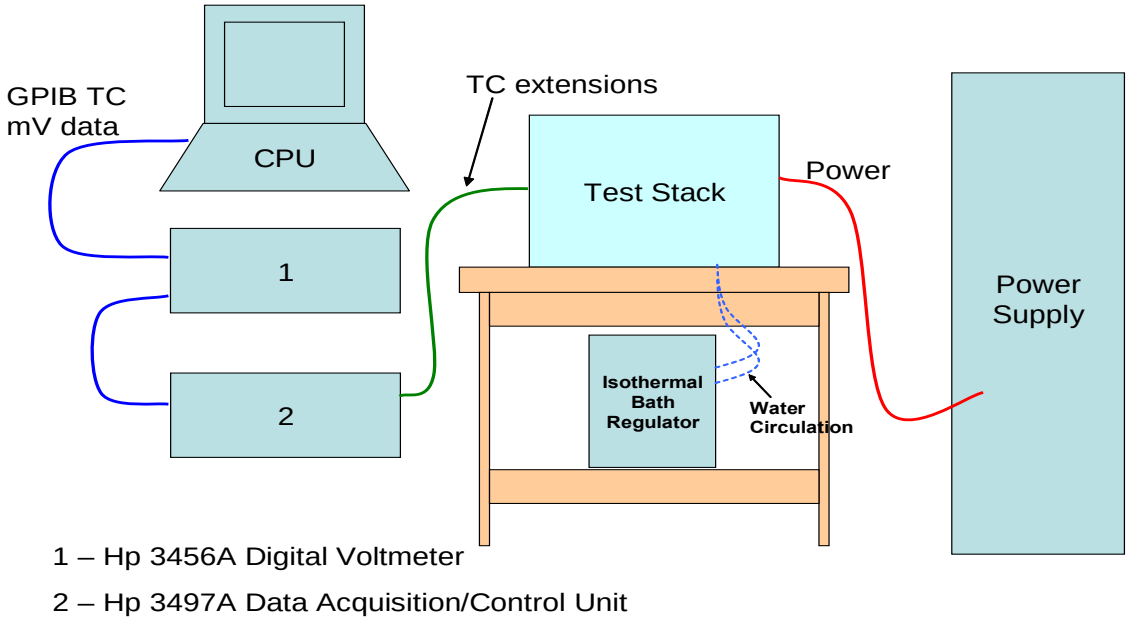

Figure 4.1: Schematic of the equipment setup

When the test was started, the guard heaters were left turned off to measure the lateral heat losses. Then, judgments were made as to how much heat was to be supplied by the guard heaters to achieve longitudinal heat flow to the desired percentage (~90-95%) of the total main heater input so that the heat transfer through the sample was approximately one-dimensional. Careful consideration was given to ensure that the guard heaters were not adding heat to the stack, i.e., the net heat flow laterally could not be into the stack.

With steady state reached, the conduction equation involving temperature difference across the sample, the dimensions of the sample, and the heat flow (1-D) through the sample was used to calculate the thermal conductivity of the sample at the mean temperature (average of temperatures on both sides of the sample). The recorded temperatures across the sample were used to produce an average temperature difference

(ΔT). The area and thickness of the sample were already known. The main concern regarding accuracy of the measurement was to ensure that the heat flow through the sample was one-dimensional. One way to do this was to calculate the heat transfer rate through each of the two reference plates on either side of the test sample, where the average of the two rates was assigned as the rate through the sample. The values of thermal conductivity for the reference material (from literature), the measured temperature difference across the reference plate, and the thickness and cross-sectional area of the reference plate were used to calculate the heat flowing through each reference plate. If the heat transfer rates through the two reference plates were equal, then one could infer that the heat transfer was one-dimensional.

Another way to estimate 1-D heat flow was to calculate the heat transfer rate into the test sample was to subtract the total heat loss from the supplied heater power. If the temperatures of the thermocouple probes along each of the surfaces of the reference plates were very close, and the temperature drop across the four lateral instrumented insulation layers was small, then the resultant heat transfer to the sample can be considered to be one-dimensional. This method required the lateral temperature differentials across the 1" insulation layers across a 0.5" piece of insulation placed on the back of the main heater (shown in Figures 3.1, 3.2), the thermal conductivity values of the insulation as a function of temperature, the distance between the thermocouples across the insulation, and an estimation of the effective area through which heat loss occurred. The manufacturer of the Fibercraft insulation provided thermal conductivity values that were fit to a quadratic curve to obtain the functional relationship of thermal conductivity to temperature. The curve fit is shown in Figure 4.2.

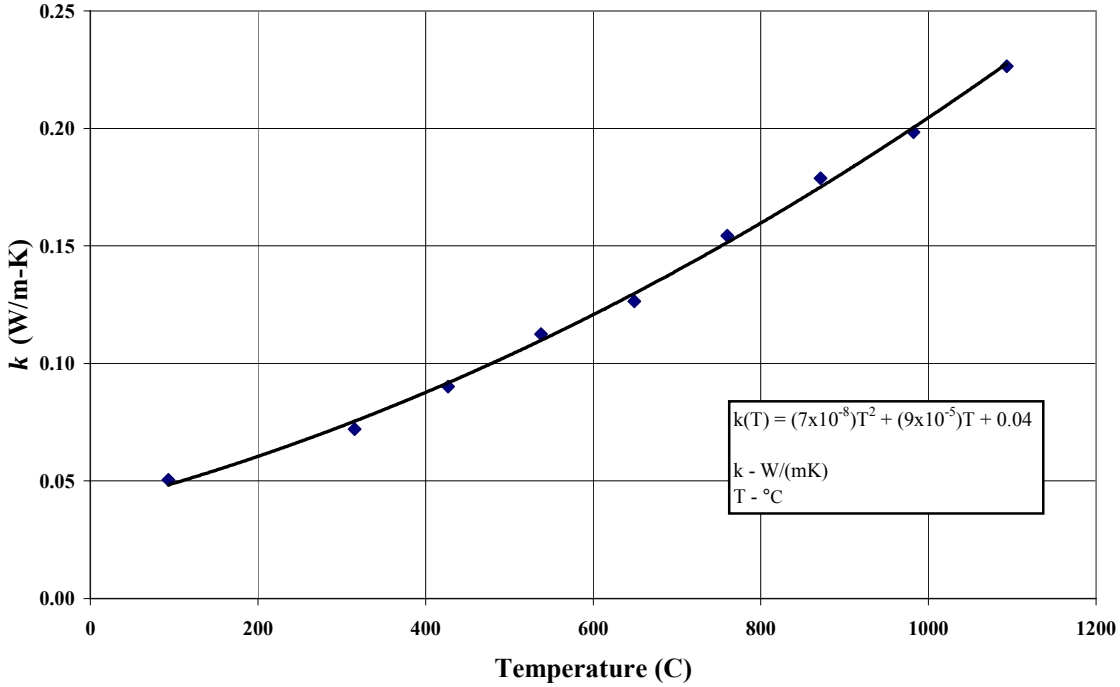

Figure 4.2: Fibercraft insulation thermal conductivity versus temperature

Careful consideration of the effective insulation area calculations is critical and will be discussed later in this chapter. The calculated heat loss essentially consisted of the four lateral directions and the direction through the back of the main heater. This method of estimation depended on the accuracy of the reported thermal conductivity of the insulation.

In order to determine which method would be implemented into the data reduction process, the one-dimensional heat flow through the test sample was calculated by both methods for the test runs. A table of the results of these two methods for the final thermal conductivity results is shown in Appendix B, in Table B.3. The second method produced lower results than the first method. The heat transfer rates calculated by

subtracting the heat losses from the main heater supply were, on average, 19% lower than the rates calculated by averaging the reference plate heat transfer rates, which indicated that only one method could be used for data reduction. The method of subtracting heat losses from the main heater supply was implemented into the data reduction because the thermal conductivity information provided by the insulation manufacturer was more reliable than the values obtained for stainless steel. The attachment of the thermocouples to the reference plates, which required a high temperature paste to secure their positions, interfered with the surfaces of the stainless steel. This interference resulted in more uncertainty that the actual thermal conductivity of the reference plates was equal to the values of stainless steel given by literature [3]. Also, the heat transfer rates calculated through the reference plates (q_{R1}, q_{R2} in Table B.3) differed from one another by as much as 14% in many cases, indicating that the designation of the average of the two rates to be the rate through the test sample would not be an acceptable assessment. Thus, the use of the reference plates to calculate heat transfer rate through the sample was less reliable. For the test runs, the reference plates acted strictly as instrumentation devices applied on both sides of the sample.

4.1: Effective Area Estimation

The effective area through which the heat loss (laterally and through the back of the heater) occurs was estimated. Temperature differentials were measured across a layer of insulation displaced 1 inch (laterally) from the stack in the four lateral directions. An appropriate lateral effective area was a projected area at the location of the differential temperature measurement, calculated using geometric similarity rules. The lateral

effective area for all four sides of the stack was calculated to represent the lateral area of the plane midway between the differential thermocouples, perpendicular to the heat flow direction. The projection increases the length considered in the area calculation from the stack length, as shown in Figure 4.3.

The height used in the lateral effective area calculation was determined to be the combined thicknesses of the spreader and instrumented plate. Using a control volume and energy balance on the stack, as shown in Figure 4.4, a reasonable choice for the lateral effective area was to consider only the spreader and instrumented plate thicknesses. The effective area for the back of the main heater direction, upon observing Figure 4.4, was estimated to be the cross-sectional area of the back surface of the heater. The potential heat loss through the sides of the main heater was neglected.

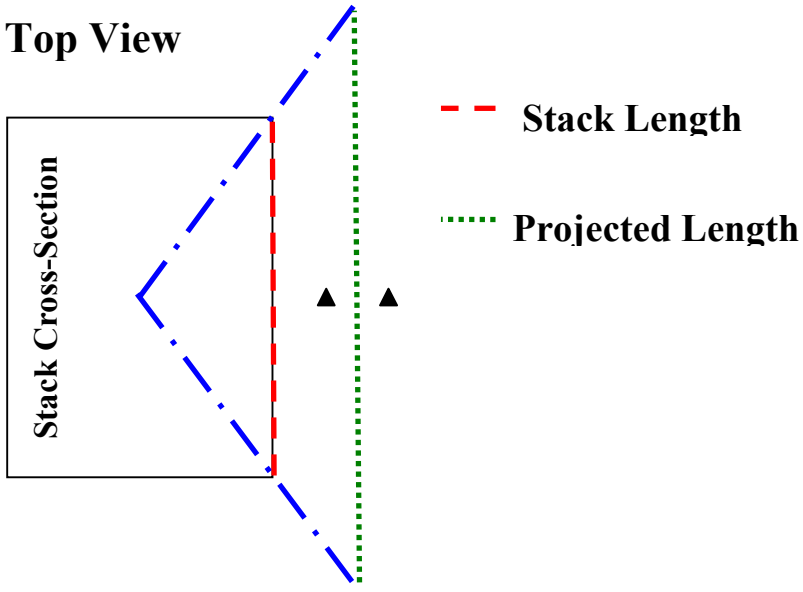

Figure 4.3: Projected area through differential thermocouples

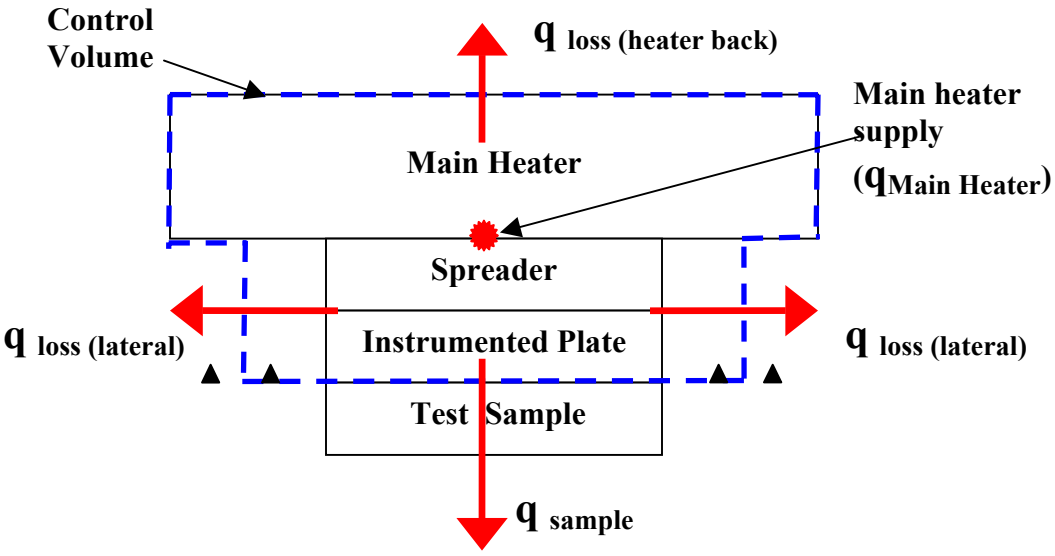

Figure 4.4: Stack control volume and energy balance

4.2: Logging of Temperature Data

For every test run, an HP VEE program recorded all relevant data from the thermocouples located throughout the experiment apparatus. Screenshots of a typical test run are shown in Figures 4.5-4.7. The figures only represent a typical run; the specific run shown in these figures was not necessarily part of the final set of results.

The alphanumeric boxes in Figure 4.5 show the result of the conversion of thermocouple emf output to a temperature value in degrees Celsius. The titled boxes (R1CL, R2HS, etc.) indicated the temperatures of the six-thermocouple locations on the instrumented/reference plates.

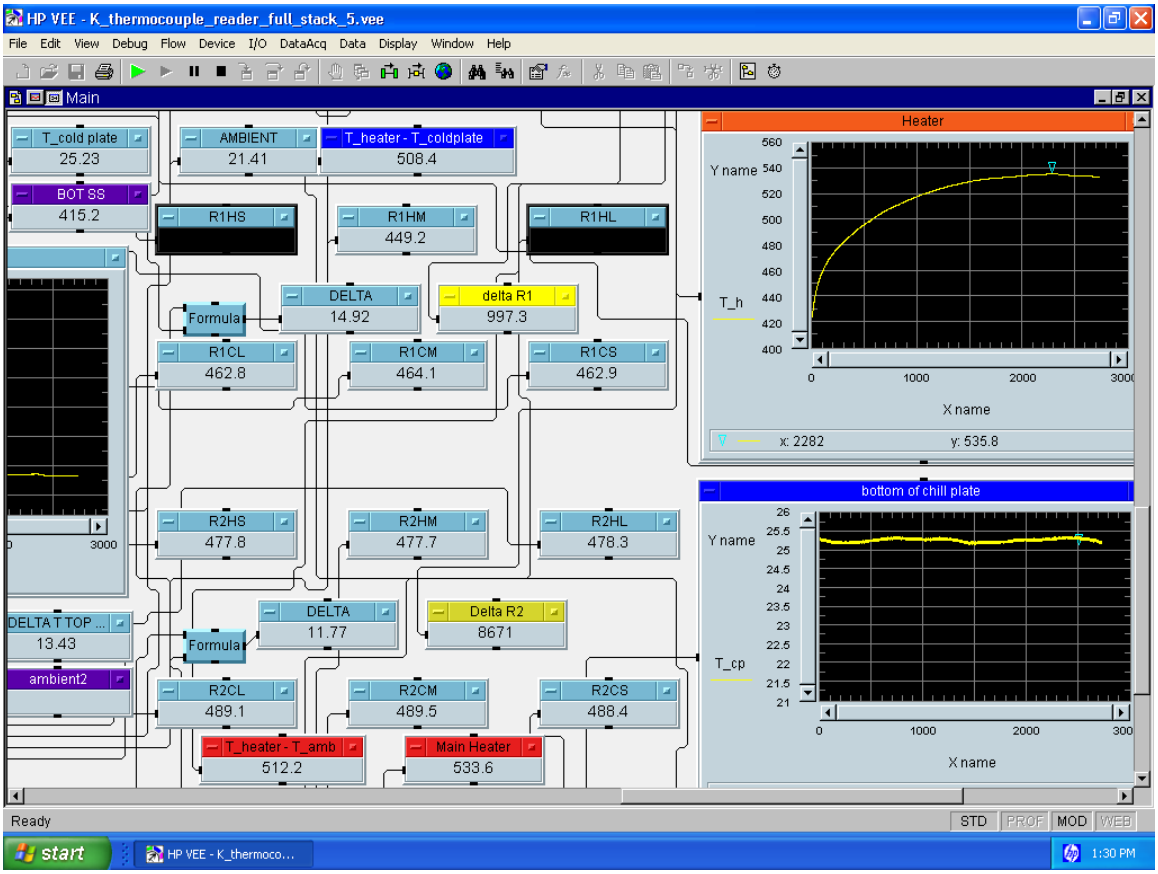

Figure 4.5: Thermocouple temperature display

Temperature uniformity on each of the surfaces of the reference plates can be monitored by observing the temperatures in Figure 4.5. A diagram of the locations of these thermocouples is provided in Appendix B. Main heater temperature and isothermal chill plate (T_cold plate) temperature are also displayed, although plots could be generated for any specific thermocouple location of interest. The temperatures were recorded in the data reduction file (Excel sheet) when the system reached steady state.

The plot windows in Figure 4.6 display temperatures in degree Celsius as the dependent variable against time, the independent variable. These four plot windows do

not represent all of the HP VEE plots utilized during the runs. The "delta samp" plot at the top left corner of Figure 4.6, for example, shows the temperature difference between the middle thermocouples on either side of the test sample. The temperatures from those thermocouples are plotted separately to the right. These plots provided a visual aid to understand the behavior of the system as a function of time, so that the system could be accurately judged to be at steady state. When the temperature values reached constant values, as seen in the plots, steady state was reached.

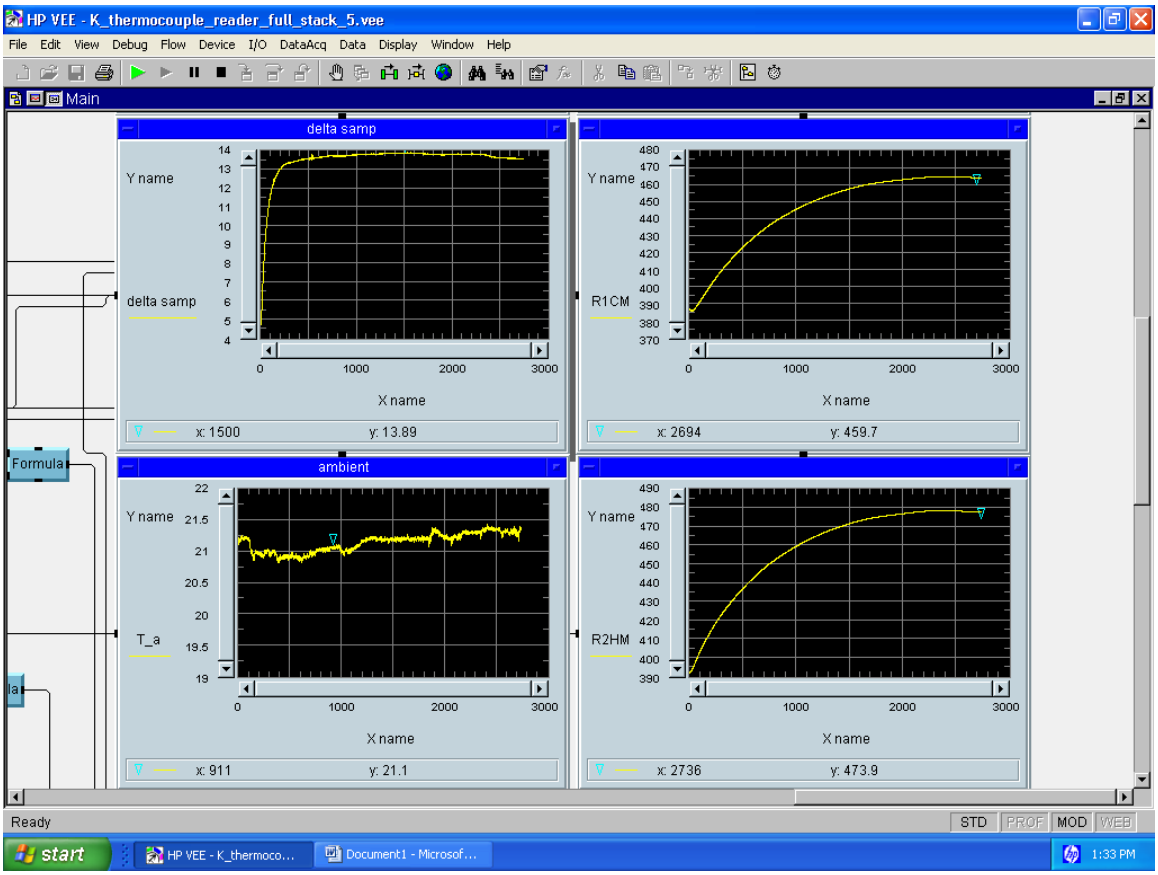

Figure 4.6: Representative temperature plots (vs. time) of stack thermocouples

The four plots in Figure 4.7 display the temperature difference (emf) across 1” of insulation placed on the four sides of the stack. The differential thermocouples on either side of the layer of insulation for all four sides of the stack were displaced 1” from the stack in the lateral direction, with lateral guard heaters placed around them. The voltages were manually converted to degree Celsius numbers by use of the appropriate thermocouple table. The plots helped to visualize a steady state pattern. The temperature differentials were used to estimate lateral heat loss, which then were used to estimate the amount of power to supply through the guard heaters.

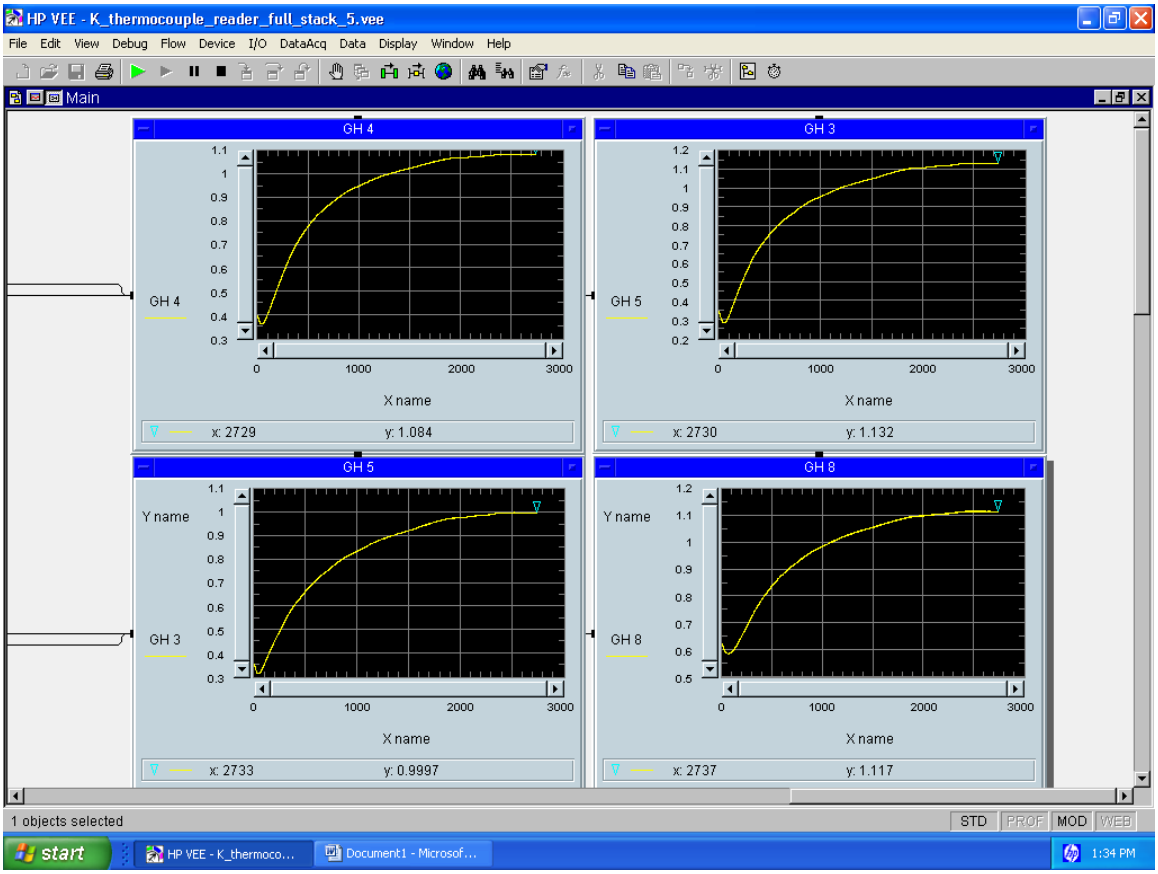

Figure 4.7: Temperature differentials across lateral insulation

Thus, the lateral heat losses were kept within a reasonable amount by monitoring the displays. Using this program, many additional aspects of the experiment could be monitored including main heater power input. It is very important that the designer of the experiment brainstorm about which information would be critical to have during the experiment, since many experimental problems could be diagnosed through observation of the data output. For instance, if the thermocouple readings were fluctuating, it would be important to check the behavior of the power supply, as it may be fluctuating with the same frequency. Systematic and organized labeling of the thermocouples based on their position in the apparatus was essential for correct programming.

4.3: Reduction of Steady-State Data

Once HP VEE displayed the steady state behavior of the system, the steady state data were entered into a Microsoft Excel program to determine the thermal conductivity of the sample at the particular temperature. Figures 4.8 – 4.10 are screenshots of the data reduction process in Excel; however the actual numbers seen in the screenshots do not necessarily represent any numbers from the final reported results. First, the temperatures of the thermocouples in the stack were recorded into a virtual stack representation in the Excel program, as shown in Figure 4.8. The program calculated temperature difference (ΔT) and provided a visual representation of the temperatures throughout the system. The temperature difference across the sample was calculated by averaging the three temperatures on the reference plate surfaces on either side of the test sample.

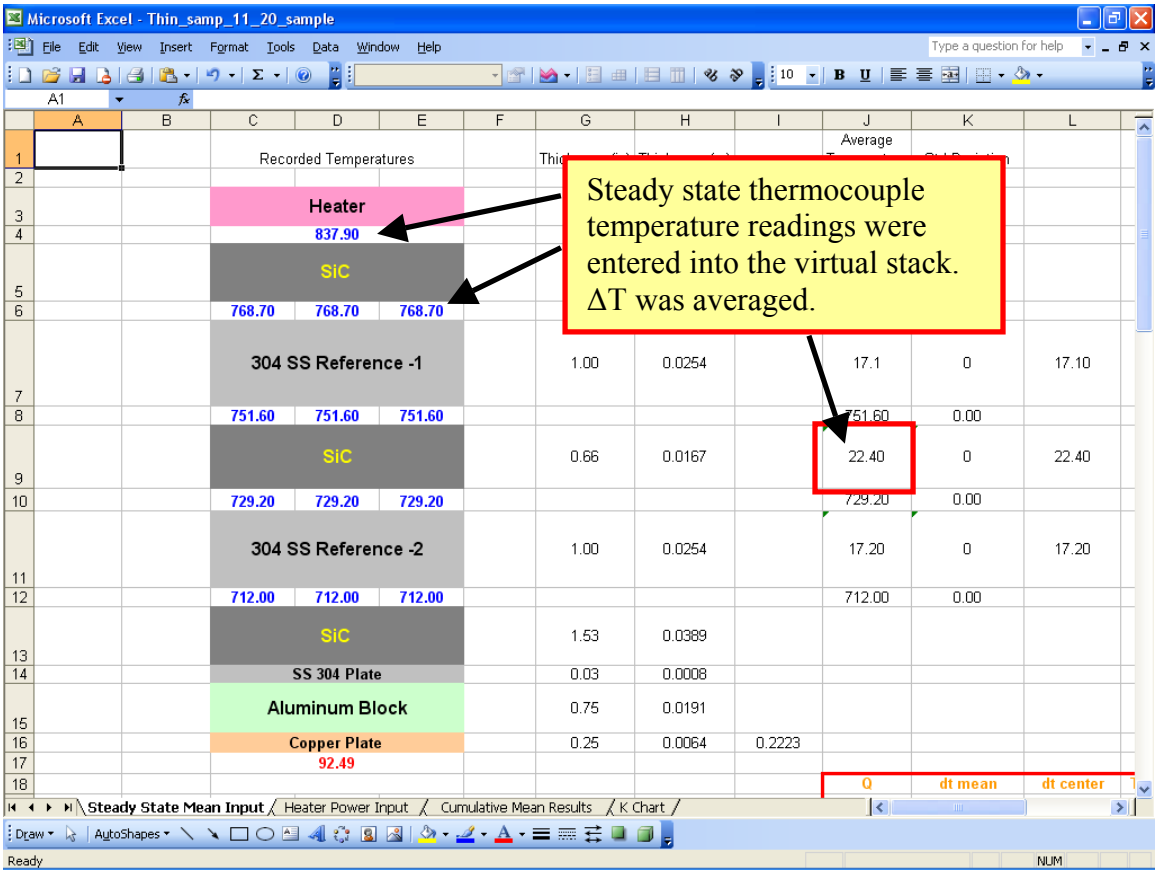

Figure 4.8: Steady state temperature input

The voltage, current, and power values for all of the heaters were recorded along with the temperature differentials in the five specified directions. The HP VEE program provided the temperature differentials, while a hand-held multimeter provided the voltage and current data from the power supply. Heat loss was calculated with the temperature differentials across the insulation and the estimations of effective area, thickness, and thermal conductivity of the insulation through which the temperature differential values were measured. The loss terms (in watts) through the back of the main heater and four sides of the stack were subtracted from the main heater wattage to calculate the heat flow

through the sample, i.e., one-dimensionally. Figure 4.9 shows the layout in the Excel program.

Essential to the calculation of thermal conductivity are the stack heat flow (q), the temperature difference across the sample (ΔT), and the physical dimensions of the sample (thickness, Δx, and cross-sectional area, A). These previously calculated numbers were entered into a separate Excel sheet (within the same Excel file) to calculate the thermal conductivity using Fourier's law for one-dimensional heat conduction. Shown in Figure 4.10, mean sample temperature and thermal conductivity for the test run were recorded along with each previously saved run. Dates and descriptions of each run were also helpful logging tools for future observation. The cumulative thermal conductivity results were plotted against sample mean temperature.–

All of the time dependent data associated with a particular test run was stored by the HP VEE program. Furthermore, after an individual file was saved, a new file name was entered into the HP VEE program so that the data from the next run could be logged into the new file. Thus progressive runs were saved under new file names, while the data acquisition and monitoring functions of the program remained the same. For each run, the steady state values were entered into the Excel data reduction program to generate the results.

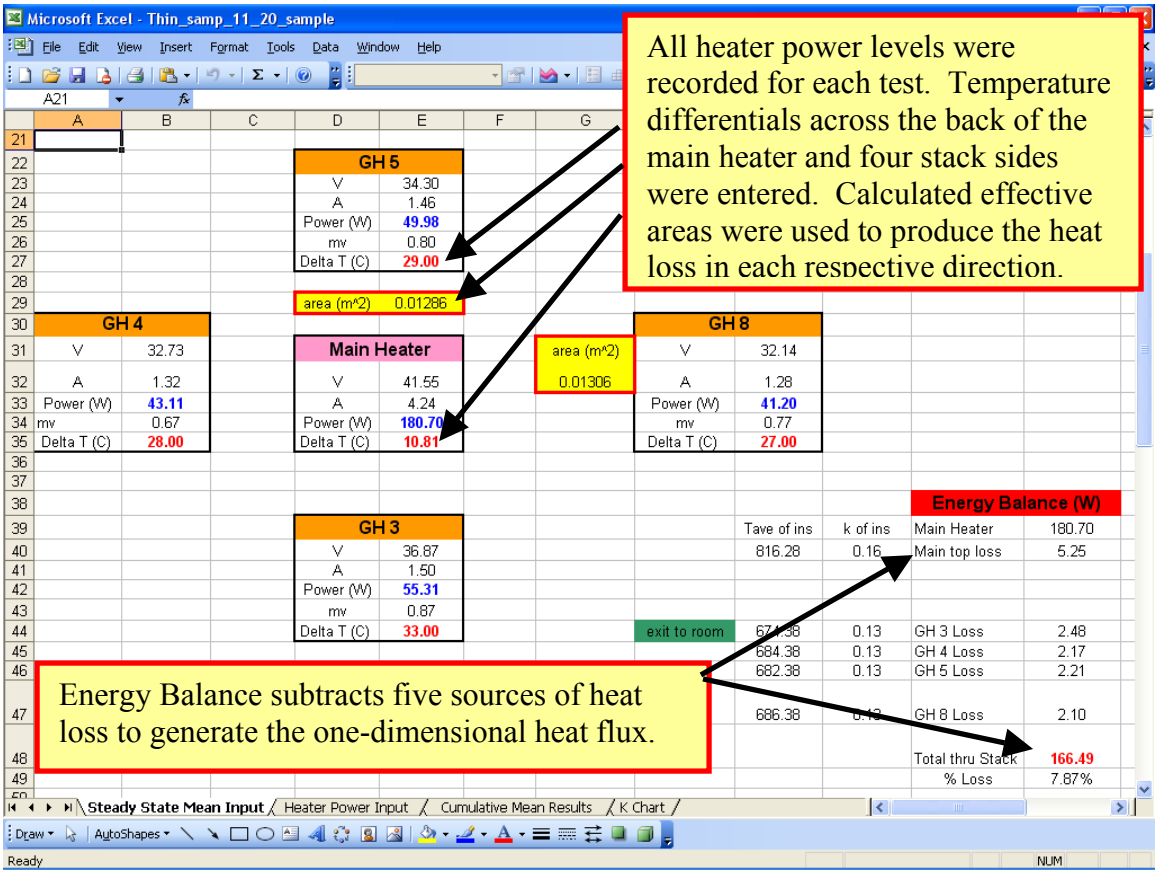

Figure 4.9: Calculation of heat flow through stack

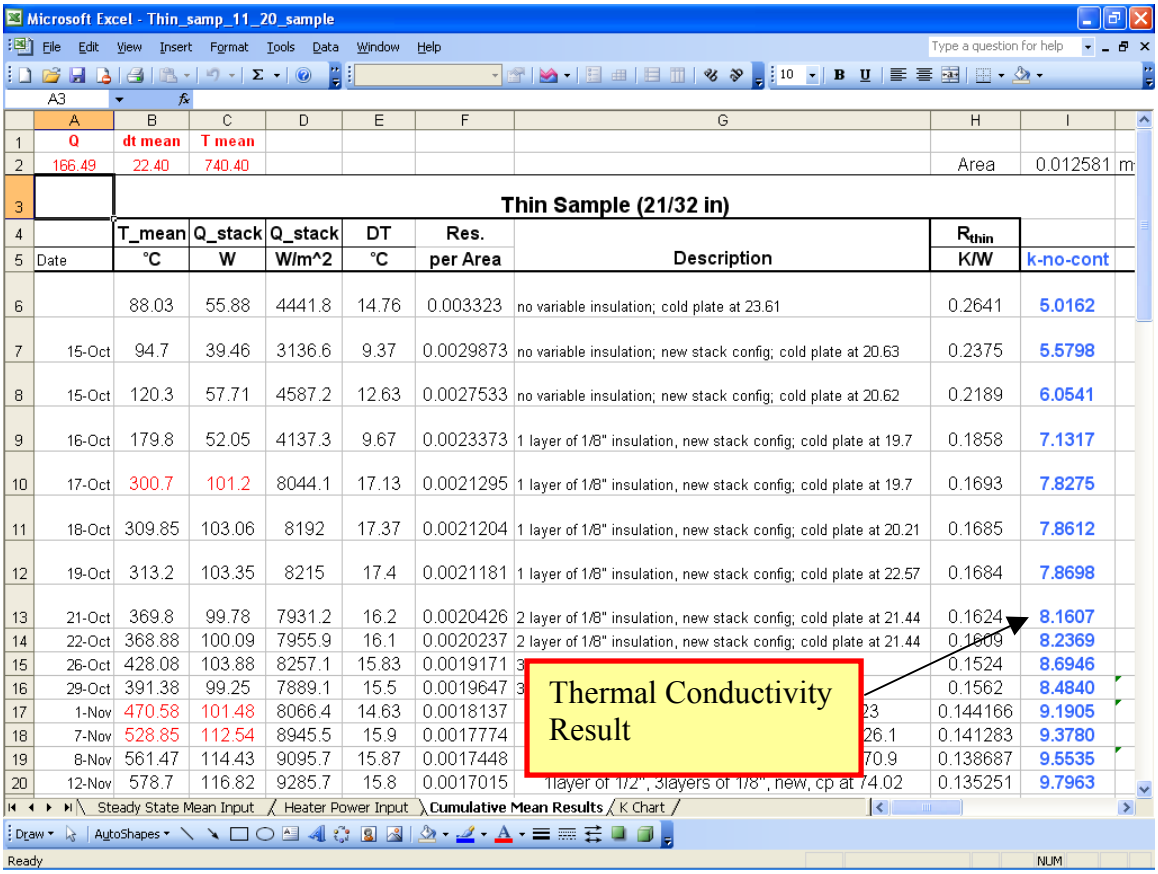

	A	B	C	D	E	F	G	H	I
1	Q	dt mean	T mean						
2	166.49	22.40	740.40					Area	0.012581 m
3		Thin Sample (21/32 in)							
4		T_mean	Q_stack	Q_stack	DT	Res.		R_{thin}	
5	Date	°C	W	W/m^2	°C	per Area	Description	K/W	k-no-cont
6		88.03	55.88	4441.8	14.76	0.003323	no variable insulation; cold plate at 23.61	0.2641	5.0162
7	15-Oct	94.7	39.46	3136.6	9.37	0.0029873	no variable insulation; new stack config; cold plate at 20.63	0.2375	5.5798
8	15-Oct	120.3	57.71	4587.2	12.63	0.0027533	no variable insulation; new stack config; cold plate at 20.62	0.2189	6.0541
9	16-Oct	179.8	52.05	4137.3	9.67	0.0023373	1 layer of 1/8" insulation, new stack config; cold plate at 19.7	0.1858	7.1317
10	17-Oct	300.7	101.2	8044.1	17.13	0.0021295	1 layer of 1/8" insulation, new stack config; cold plate at 19.7	0.1693	7.8275
11	18-Oct	309.85	103.06	8192	17.37	0.0021204	1 layer of 1/8" insulation, new stack config; cold plate at 20.21	0.1685	7.8612
12	19-Oct	313.2	103.35	8215	17.4	0.0021181	1 layer of 1/8" insulation, new stack config; cold plate at 22.57	0.1684	7.8698
13	21-Oct	369.8	99.78	7931.2	16.2	0.0020426	2 layer of 1/8" insulation, new stack config; cold plate at 21.44	0.1624	8.1607
14	22-Oct	368.88	100.09	7955.9	16.1	0.0020237	2 layer of 1/8" insulation, new stack config; cold plate at 21.44	0.1609	8.2369
15	26-Oct	428.08	103.88	8257.1	15.83	0.0019171	3	0.1524	8.6946
16	29-Oct	391.38	99.25	7889.1	15.5	0.0019647	3	0.1562	8.4840
17	1-Nov	470.58	101.48	8066.4	14.63	0.0018137	23	0.144166	9.1905
18	7-Nov	528.85	112.54	8945.5	15.9	0.0017774	26.1	0.141283	9.3780
19	8-Nov	561.47	114.43	9095.7	15.87	0.0017448	70.9	0.138687	9.5535
20	12-Nov	578.7	116.82	9285.7	15.8	0.0017015	1layer of 1/2", 3layers of 1/8", new, cp at 74.02	0.135251	9.7963

Figure 4.10: Cumulative display of results

Chapter 5. Experimental Results

During the course of the experiment, the results were recorded and accumulated. There were several phases of the experiment, due to design changes. The ultimate objective throughout the entire process was to generate steady state thermal conductivity values up to a mean sample temperature of 1000ºC and observe a functional relationship between thermal conductivity and temperature. Issues such as having adequate insulation and guarding and maintaining a constant power source greatly affected the system operation. Initially, samples of two different thicknesses (referred to as thick and thin samples) were tested using configuration A. Results were obtained for the thick sample until it was determined that the ability to provide adequate heating by the lateral guard heaters for the thick sample was limited. The thick sample is about three times the thickness of the thin sample. This, combined with the low thermal conductivity of the sample material made it difficult to maintain one-dimensional heat flow, since the larger lateral area of the thick sample resulted in higher potential for lateral heat losses. Further, when variable insulation was added to the stack, the mean sample temperature did not sufficiently increase, indicating that only additional power supply to the heater would be able to drive the experiment to higher temperatures. The amount of heat loss generated as a result of higher heater power supply was too significant to achieve higher temperatures with the thick sample. Therefore, the thin sample was exclusively used throughout the rest of the testing, and configuration B was designed to achieve high temperatures. This design was successful in achieving higher temperatures by the additional guard heaters and by replacing the copper chill plate with a “cold side” heater.

The "cold side" heater was controlled such that the stack temperatures could be elevated without significantly increasing the power to the main heater. The gist of the approach of using the "cold side" heater was to achieve the desired sample temperatures with relatively low power supply to the system, and yet maintain a low temperature difference across the sample. In order to reduce the heat loss to the surroundings further and greatly limit the unaccounted sources of heat loss, fiberglass batting was added around the stack. The chronological display of results for each implemented design is provided in Appendix A.

5.1: Final Set of Results

The final design (from configuration B) that included the fiberglass batting produced the most reliable results. The guarding was adequate, reaching high temperatures (>500ºC) was feasible, and the estimation of heat loss was the most accurate due to the presence of the fiberglass batting. Thus, these results were chosen over the results from the previous designs. All relevant data for these results are presented in Appendix B, Tables B.1 and B.2. Figure 5.1 is a plot of this set of results of thermal conductivity versus mean sample temperature. The thermal conductivity ranged from about 5 W/(m K) at 200 ºC to about 9.5 W/(m K) at 860 ºC. It should be noted that in the runs with guard heaters turned on (Table B.2), the percent of total heat loss relative to the power supply to the main heater ranged between 4.75 and 9.61%. Since the losses were kept below 9.61% for these runs, it can be concluded that the heat transfer through the sample is mostly one-dimensional. As the mean temperature approached 800ºC, the results began to scatter between 9 and 10 W/(m K). This was due to the difficulties in

obtaining consistent results at very high temperatures. It was found that the power to the heaters could not be kept constant long enough to achieve a steady state condition because of fluctuating line voltage. Providing substantial guarding to limit the heat transfer through the stack to one dimension while using a "cold side" heater to increase the stack temperature also posed problems. The "cold side" heater serving as a heat sink was not as effective as the copper chill plate, which was operating at a much lower temperature. However, reaching higher temperatures would not have been possible without replacing the chill plate with the heater.

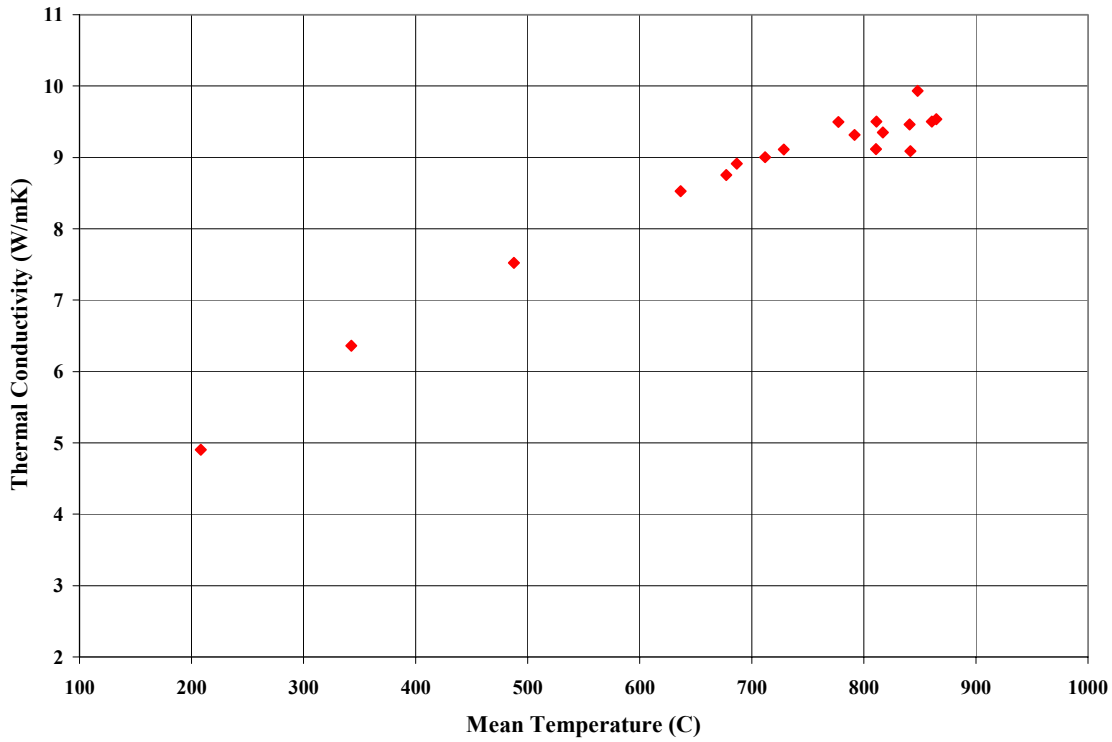

Figure 5.1: Thermal conductivity of thin sample vs. temperature for configuration B with added fiberglass batting

Upon reaching higher temperatures, one must consider the possible power fluctuations associated with voltage fluctuations, which at times occurred at an amplitude of at most 1% of the average applied voltage, with a period of about 12 hours. These slowly oscillating voltages, although they produced inconsistent results, may be considered to result in a quasi-steady state for the system. For a confirmation of the results at the higher temperatures, several of the runs were repeated.

A cubic polynomial curve fit to the final set of results is shown in Figure 5.2. The curve fit equation is shown in Equation 2, where k (W/(m K)) is the sample thermal conductivity and T (°C) is the mean sample temperature. The average deviation of the data from the curve fit (at corresponding temperatures) was about 2.5% of the curve fit values.

$$k(T) = -\left(2\times10^{-9}\right)T^3 - \left(4\times10^{-6}\right)T^2 + 0.0128T + 2.44 \qquad (2)$$

for $208°C \le T \le 865°C$,

$4.90\text{W/(m K)} \le k \le 9.93\text{W/(m K)}$

The results were calculated based on the difference between the average of the three temperatures on either side of the test sample. The one-dimensionality of the heat transfer through the sample can be observed by re-calculating the thermal conductivity results based on the difference between the temperatures at the center of the cross-section on either side of the test sample. If the average results are equal to the centerline results, the temperature is uniformly distributed along the cross-section, and the heat transfer is considered to be one-dimensional. The centerline results were calculated and plotted with the average temperature difference results in Figure 5.3. The centerline results are

nearly equal to the average results, indicating the one-dimensionality of the conduction through the sample.

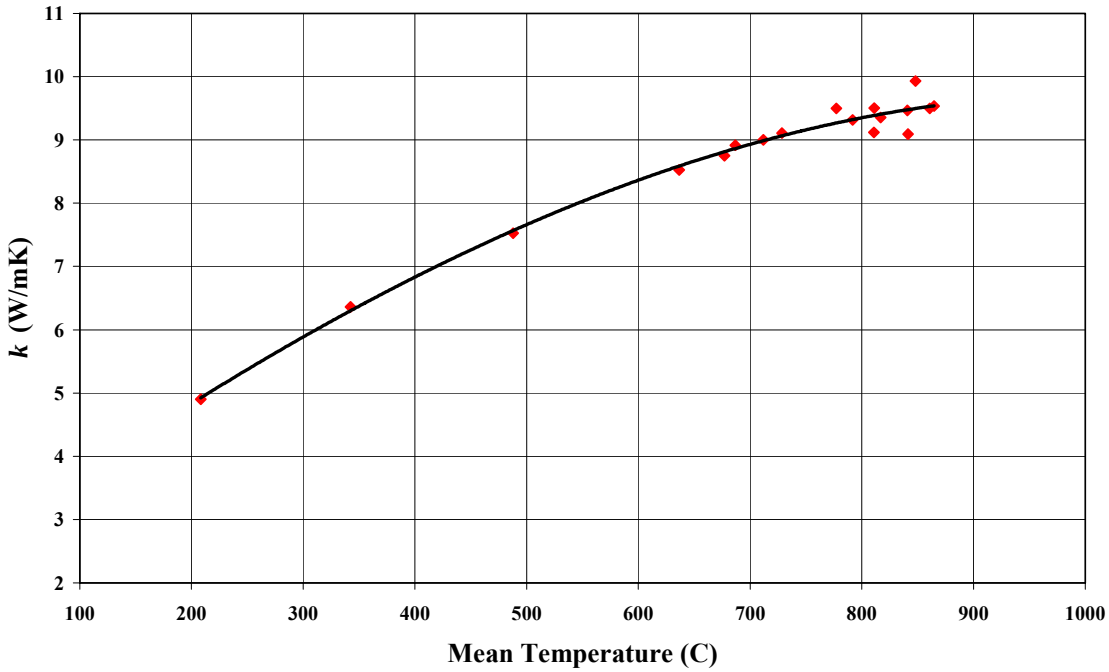

Figure 5.2: Cubic curve fit to thermal conductivity data

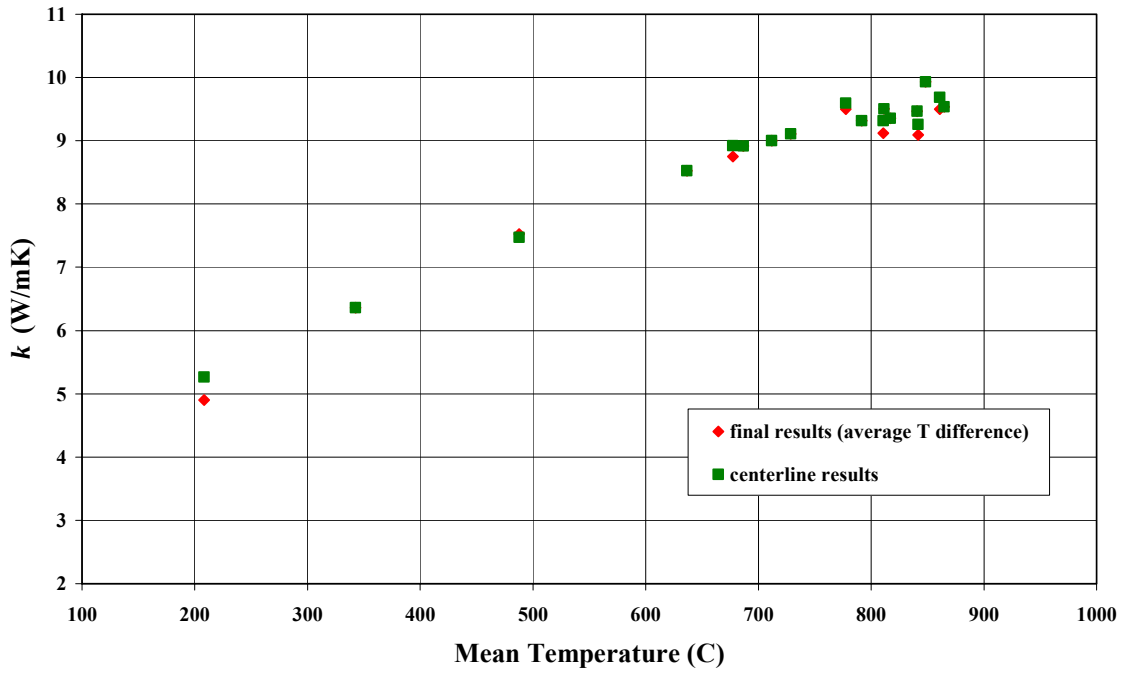

Figure 5.3: Comparison of average results and centerline results

5.2: Independent Evaluation of the Reasonableness of Measured Values of Thermal Conductivity

The stack thermal conductivity values were 9 ~ 10 W/(m K) for temperatures near 800°C as opposed to the published values for pure silicon carbide of 87 W/(m K) at 800°C [3]. The measured thermal conductivity values are an order of magnitude smaller than those for pure silicon carbide. However, since silicon carbide comes in numerous compositions, it is difficult to compare the obtained values with published values. To be sure about the order of magnitude of the measured values, a simple test, independent of the stack tests, was conducted utilizing the concept of heat propagation to estimate thermal conductivity. The equation for heat propagation in Equation 3 relates the

penetration depth of the heat wave through the material to the time for the heat wave to travel the penetrated distance [4].

$$\delta = c\sqrt{\alpha t} \tag{3}$$

Knowing the depth and recording the time, thermal diffusivity was solved. Then, thermal conductivity was estimated using the approximate density and specific heat of the material, as shown in Equation 4.

$$\alpha = \frac{k}{\rho C_P} \tag{4}$$

Simple tests were performed on the 21/32" (thin) test sample and a 1" thick instrumented stainless steel plate. The sample was placed on a hot plate, and a thermocouple was used to record the temperature on the opposite side of the sample. A stopwatch was used to record the time for the temperature on the opposite side to change by a specified amount (0.1ºC). The same test was performed on the stainless steel plate. The recorded times for the heat wave to propagate through both materials were both approximately 14 seconds, although the depths were different for the two materials. The reduction of the propagation equations for both materials is shown in Equation 5.

$$\frac{\delta_{SS}}{\delta_{SiC}} = \frac{c}{c}\sqrt{\frac{\alpha_{SS} t_{SS}}{\alpha_{SiC} t_{SiC}}} = \sqrt{\frac{\alpha_{SS}(14s)}{\alpha_{SiC}(14s)}} = \sqrt{\frac{\alpha_{SS}}{\alpha_{SiC}}} \tag{5}$$

where δ_{SS} = 1", δ_{SiC} = 21/32", α_{SS} = 3.95x10^{-6} m^2/s

Substituting in the respective thicknesses and the thermal diffusivity of the stainless steel from literature, the thermal diffusivity for the test sample was determined. Then, using silicon carbide values (from the literature) of density (3160 kg/m^3) and specific heat (675 J/(kg K)) [3] as estimations for the test sample, the thermal conductivity was determined to be approximately 3.6 W/(m K), at a mean temperature of about 40ºC.

The value of thermal conductivity from the stack was 5 W/(m K) at a mean temperature of 200ºC, and it decreased with decreasing temperature. By linearly extrapolating the first four data points in Figure 5.1, the estimated thermal conductivity at a mean temperature of 40ºC based on the stack tests is about 3.65 W/(m K). Therefore, the test results for the sample obtained through the stack experiment were judged to be reliable by this independent test.

Chapter 6. Uncertainty Analysis

As with any experimental procedure, uncertainty in the final results must be addressed. The accuracy of the results depended on the accuracy of the utilized instruments, such as thermocouples, voltmeters, and power supply. The individual measurement uncertainties could be used to generate an overall thermal conductivity uncertainty by use of the Kline-McClintock method shown in Appendix C. These individual uncertainties consisted of the sample thickness (Δx), sample cross-sectional area (A), the temperature difference across the sample (ΔT), and the one-dimensional heat transfer rate through the stack (q). The equations for these individual uncertainties are provided in Appendix C. Since thermal conductivity was calculated with these four individual values, thermal conductivity uncertainty (ω_k) was affected by these four individual uncertainties. Thus, minimizing the instrumental uncertainties produced more accurate thermal conductivity results. The sample thickness and cross-sectional dimensions were measured with a caliper of 0.001" uncertainty. The thermocouple uncertainty for a single temperature measurement was 0.3ºC.

6.1: Heat Transfer Rate Uncertainty

The uncertainty for the heat transfer rate through the stack was calculated by applying the Kline-McClintock method further, as seen in Appendix C. This calculation consisted of the voltage and current readings from a voltmeter for the main heater, the dimensions of the effective areas used in heat loss calculations, the temperature differentials across insulation for the four lateral directions and back of main heater direction, the thickness of the insulation across which the temperature differentials were

recorded, and the thermal conductivity of the insulation. The uncertainties for all of these quantities were also required. Voltage and current uncertainty, based on the voltmeter/multimeter equipment, were 0.5% of the voltage reading and 1% of the current reading, respectively. The dimensions of the effective areas for each heat loss direction and the thickness across the temperature differential thermocouples were based off of estimations. For instance, the insulation thickness dimension was not as clearly known as the sample thickness dimension because the distance between the differential thermocouples varied due to the compression of the stack during testing. Furthermore, the effective area dimensions were based off of educated estimations, rather than actual measurable quantities. Therefore, the length measurement uncertainty was kept at 1/64".

The uncertainty of the thermal conductivity of the insulation provided by the manufacturer was also determined. The average difference between the actual given thermal conductivity values and the quadratic curve fit values at the same corresponding temperatures (from Figure 4.2) was taken to be the uncertainty, which was 0.0037 W/(m K).

6.2: Uncertainty Results and Additional Considerations

The thermal conductivity uncertainties were calculated for each run, and the results are plotted with the appropriate error bars in Figure 6.1. The uncertainty results are tabulated in Appendix C. In Figure 6.1, the error bars in the y-direction represent the thermal conductivity uncertainties, which maximized at about ±0.35 W/(m K). The average uncertainty was about ±3% of the thermal conductivity results.

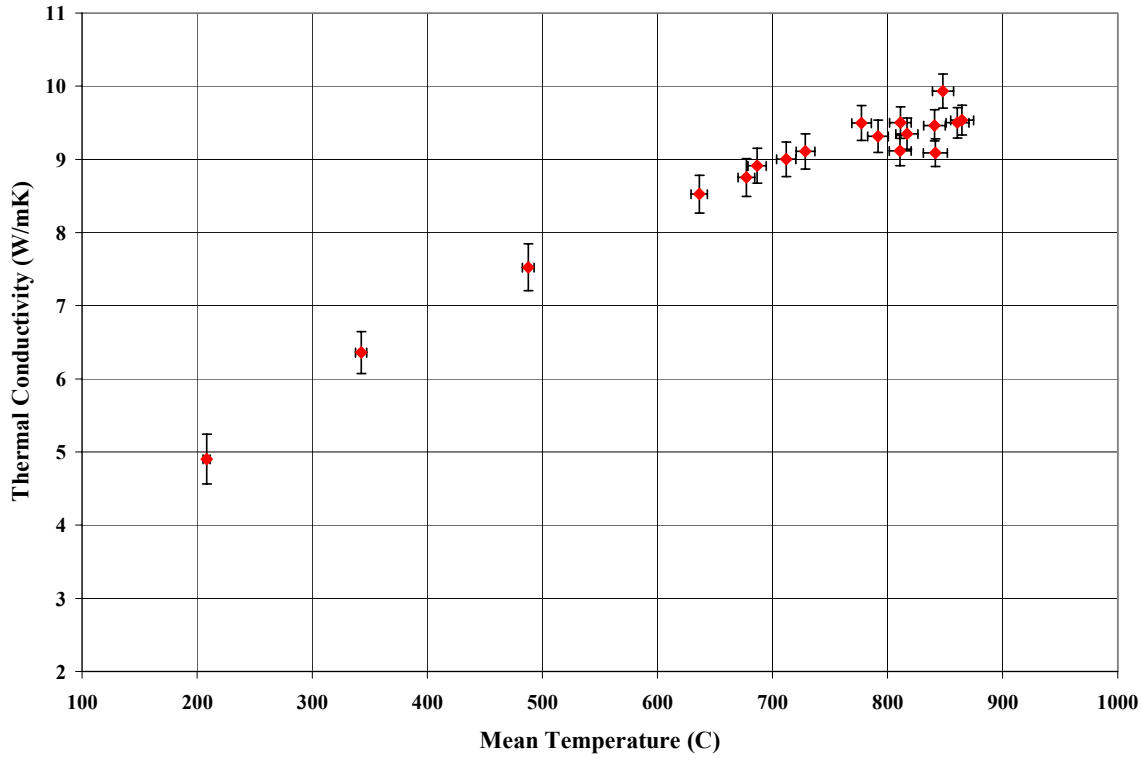

Figure 6.1: Sample thermal conductivity as a function of temperature with error bars

The error bars in the x-direction represent the temperature range of the test sample at each steady state condition. Based on the uncertainty calculations for each individual point, the error bars show the range in which the thermal conductivity result may lie. One important consideration for this experiment was the calculation of heat loss to the surroundings. The accuracy of this particular estimation was not clearly known, since it was neither possible to identify nor to account for every source of heat loss. However, as concluded in Chapter 4, this method of estimation was determined to be the best available for calculating heat transfer through the test sample. It should be noted that the presented uncertainty results (3% average) were based on the methodology used to estimate the

heat losses from measurements as described in Chapter 4. Though this is not actually certain, efforts were made to reduce the effect of this uncertainty in estimation on the thermal conductivity results. If the amount of heat loss for a particular test was significant, the uncertainty associated with the heat loss estimation would significantly affect the thermal conductivity result. If the heat loss was greatly reduced, the effect of this uncertainty would diminish, and the result would be more reliable. Increasing the guard heater supply to the stack as much as allowable not only reduced the heat loss and maintained one-dimensional heat transfer through the test sample, but also reduced the effect of the uncertainty behind the heat loss estimation. Other efforts to reduce heat loss, such as adding fiberglass batting around the stack, also minimized these errors.

Chapter 7. Conclusions

The thermal conductivity values for the unknown sample over a range of mean sample temperatures (208°C to 865°C) were determined experimentally by a steady-state method. The test apparatus was designed to generate an approximate one-dimensional heat flow through the sample and to achieve the desired mean sample temperatures by incorporating appropriate guarding and insulation, as well as instrumentation. Incorporating components such as variable insulation and a "cold side" heater allowed for the stack temperature to be elevated while maintaining the narrow temperature difference across the test sample. Guarding and insulation around the stack significantly limited the heat transfer to one dimension, which allowed the calculation of the sample thermal conductivity from steady state temperature measurements, the thickness and cross-sectional area of the sample, and the estimated heat transfer rate through the sample.

The sample thermal conductivity values ranged from 4.90 to 9.93 W/(m K) over the temperature range, with the thermal conductivity values displaying a cubic functional relationship to the mean sample temperature. Uncertainty was calculated for the final set of thermal conductivity results at an average of ±3% of the results.

Chapter 8. Improvements for Future Experiments

In retrospect, there are several improvements that can be made for any future thermal conductivity experiments. Installing radiation shields, such as stainless steel plates with mirror finishes, around the stack would reduce thermal radiation loss to the surroundings. This addition will greatly aid in high temperature measurements. A constant problem that was experienced at elevated temperatures was due to a fluctuating power supply, which hindered many attempts to reach steady state. Insuring a reliable, constant power supply along with an understanding of the power requirements will produce more consistent high temperature results. The heat stresses from long periods of testing began to affect the integrity of the thermocouples at high temperatures. Therefore, thicker gage thermocouples rated for the desired temperature range will eliminate the risk of thermocouples breaking during the experiment. New reference plates should be used that are designed with smaller grooves for thermocouple installation.

References

1. Tritt, Terry M. *Thermal Conductivity: Theory, Properties, and Applications.* Kluwer Academic/ Plenum Publishers. New York, 2004.

2. *Annual Book of ASTM Standards (2004), Section 14: General Methods and Instrumentation: Volume 14.02: General Test Methods; Forensic Sciences; Terminology; Conformity Assessment; Statistical Methods.* pp. 328-335. ASTM International. West Conshohocken, PA, 2004.

3. Incropera, Frank P. and DeWitt, David P. *Fundamentals of Heat and Mass Transfer, Appendix A: Thermophysical Properties of Matter.* John Wiley & Sons, Inc. 2002.

4. Ozisik, M. Necati. *Heat Conduction Second Edition.* p.329. John Wiley & Sons, Inc. New York, 1993.

Appendix

Appendix A. Description of Cumulative Results

The results from all of the test runs during the progression of the experiment are provided in Figures A.1-A.3. The results from configuration A are shown in Figure A.1.

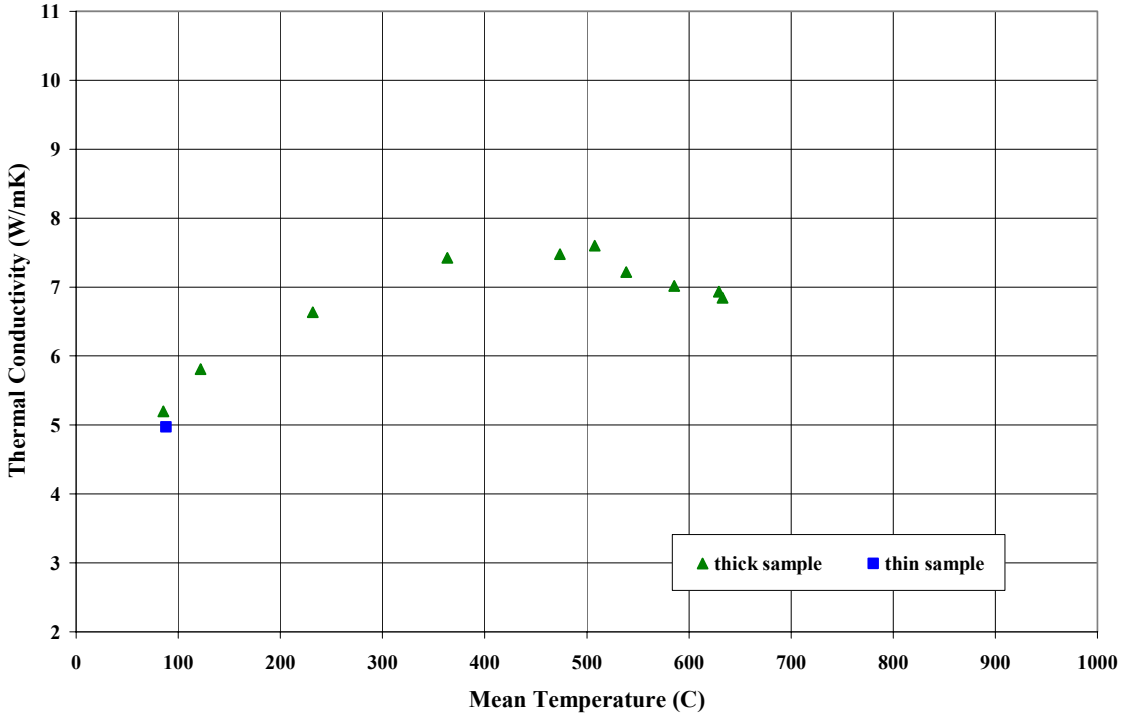

Figure A.1: Thermal conductivity results from configuration A

The results for configuration A were mostly for the thick sample. As explained in Chapter 5, there was too much heat loss through the stainless steel sheet and too large of a temperature difference across the thick sample for this design configuration to achieve higher stack temperatures. Configuration B was later developed to reach higher stack

temperatures for the thin sample only. The results from this configuration are shown in Figure A.2.

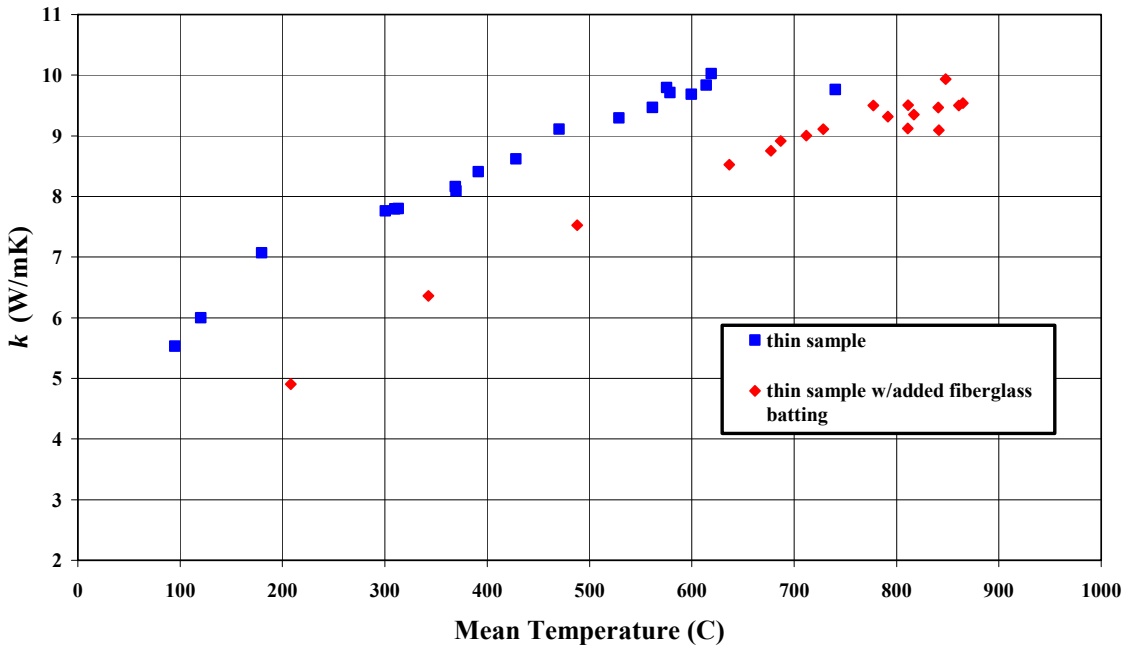

Figure A.2: Thermal conductivity results from configuration B

For configuration B, the two distinct sets of data for the thin (21/32") sample arose out of the two degrees of insulation applied to the stack. The first degree of insulation was from the original data taken with only the Fibercraft insulation around the stack (Figure 3.2). The second degree of insulation was obtained by wrapping an additional layer of fiberglass batting around the Fibercraft insulation. Recalling the explanation provided in Chapter 5, the additional insulation was applied because there was a concern that the amount of heat escaping through the various cracks of the

Fibercraft layers was too significant to neglect. The methods for determining effective area and eventually thermal conductivity were the same for both degrees of insulation.

The original case did not account for the heat loss through air gaps and cracks. Therefore, the calculation of heat loss laterally and through the back side of the heater was a low estimate, leading to a higher calculated heat flow through the stack. This high estimation of heat flow through the stack resulted in higher thermal conductivity values. The second case included the fiberglass batting. Thus, the heat loss through cracks and other sources was significantly reduced. Consequently, that amount of heat was re-directed through the test sample. The resulting calculations of heat loss laterally and through the back of the main heater accounted for nearly all of the total heat loss. The calculations of heat loss were higher than the original case and produced lower calculations of heat flow through the stack and lower thermal conductivity. The added fiberglass batting caused a significant drop in the resultant thermal conductivity. The data produced from this addition of fiberglass batting was more accurate because the added insulation significantly limited the heat loss to the lateral and back-of-heater directions only, which were accounted for in the calculations involving effective area and temperature differential.

In order to compare the results from the different configurations, the cumulative collection of all thermal conductivity results are presented in Figure A.3. The thick sample results from configuration A began to decrease as high mean sample temperatures were reached because the heat losses and the large thickness of the sample resulted in very high temperature differences across the sample. The inverse relationship between thermal conductivity and temperature difference (Equation 1) indicates that if the

temperature difference is large, as was the case with configuration A at high temperatures, the resultant thermal conductivity would be low and would continue to decrease. The thin sample results from configuration B without the fiberglass batting and some of the thick sample results at low temperatures were higher than the thin sample results from configuration B that included the fiberglass batting because the estimation of heat loss was too low. If the heat loss calculation is an underestimation, then the calculation of the heat transfer through the sample would be an overestimation. The direct relationship between heat transfer through the sample and thermal conductivity (Equation 1) indicates that the overestimation of heat transfer rate would produce an overestimation in thermal conductivity. Thus, the results presented in Figure A.3 exhibit these behaviors.

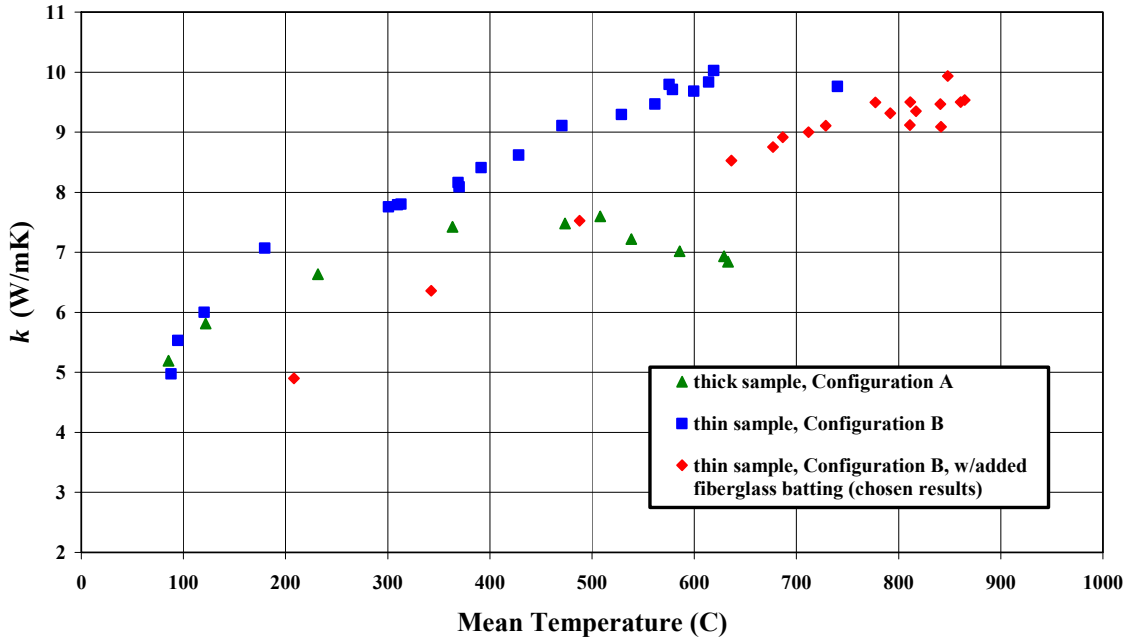

Figure A.3: Cumulative collection of results from both Configurations A and B

Appendix B. Data and Calculated Results for Final Results

Temperature Labels of Thermocouples in Stack

Main Heater, T_{MH}			T_{MH}: Main Heater temperature at surface
SiC Spreader			
R1HS	**R1HM**	**R1HL**	R1H(S,M,L*): Hot side thermocouples of first instrumented plate
304 SS Instrumented Plate -1			
R1CL	**R1CM**	**R1CS**	R1C(S,M,L*): Cold side thermocouples of first instrumented plate
SiC Test Sample			
R2HS	**R2HM**	**R2HL**	R2H(S,M,L*): Hot side thermocouples of second instrumented plate
304 SS Instrumented Plate -2			
R2CL	**R2CM**	**R2CS**	R2C(S,M,L*): Cold side thermocouples of second instrumented plate
SiC Spreader			
SS 304 Plate			
Aluminum Block*			*Not present in all runs
Chilled Copper Plate*, T_C			T_C: Isothermal copper plate temperature (or cold side temperature)

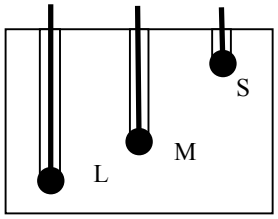

Instrumented Plate

S,M,L refer to short, medium, and long. They depict the location of the corresponding thermocouple (see left) along the diagonal of the surface of the instrumented plate.

Table B.1: Steady-State Stack Temperatures (°C)

	Heater	Thermocouples in Instrumented Plates												Cold Side
Run #	**T_{MH}**	**R1HS**	**R1HM**	**R1HL**	**R1CL**	**R1CM**	**R1CS**	**R2HS**	**R2HM**	**R2HL**	**R2CL**	**R2CM**	**R2CS**	**T_C**
1	235.9	214.9	215.5	215.2	211.1	211.2	211.7	205.1	205.4	204.8	n/a	202	n/a	182.8
2	390.5	n/a	354	n/a	n/a	347.4	n/a	n/a	337.6	n/a	n/a	331	n/a	299
3	529.5	499.9	500	499.8	493.1	493.2	492.3	482.9	483.1	482.5	n/a	476.5	n/a	437.2
4	692.9	n/a	652.7	n/a	n/a	643.5	n/a	n/a	629.4	n/a	n/a	620.2	n/a	567.3
5	736.5	694.3	694.4	694.1	684.5	684.5	n/a	669.8	670.3	669.7	n/a	660.7	n/a	613.7
6	752.1	n/a	704.7	n/a	n/a	694.7	n/a	n/a	678.7	n/a	n/a	668.7	n/a	613.1
7	779.9	n/a	731.1	n/a	n/a	720.1	n/a	n/a	703.6	n/a	n/a	692.6	n/a	629.7
8	795.8	n/a	748	n/a	n/a	736.7	n/a	n/a	720.4	n/a	n/a	709.4	n/a	659.9
9	851.7	798.4	800.7	799.2	785.2	786.4	n/a	767.9	769.5	769.4	n/a	757.5	n/a	703.6
10	869	n/a	813.7	n/a	n/a	800.7	n/a	n/a	782.7	n/a	n/a	770	n/a	714
11	888.3	833.4	834.3	833.5	819.8	820.7	n/a	800.7	802.1	801.4	n/a	789.3	n/a	733.8
12	890.3	n/a	833.7	n/a	n/a	820.7	n/a	n/a	801.9	n/a	n/a	789.2	n/a	732.2
13	895.4	n/a	839.5	n/a	n/a	826.5	n/a	n/a	807.4	n/a	n/a	794.7	n/a	737.2
14	920.2	863.3	866	864.4	849.4	851	n/a	830.2	832	832.2	n/a	819.1	n/a	761.4
15	925.1	865.8	866.9	866	851.2	852.3	n/a	830.4	831.9	831.2	n/a	818.3	n/a	758
16	925.7	n/a	871	n/a	n/a	857.4	n/a	n/a	838.9	n/a	n/a	825	n/a	769
17	940.8	884.3	886.2	884.8	869.7	871.3	n/a	849.8	852	851.5	n/a	838.2	n/a	779.7
18	946.4	n/a	889.7	n/a	n/a	874.9	n/a	n/a	854.7	n/a	n/a	840.7	n/a	781.4

Table B.2: Experimental Results (Configuration B with added fiberglass batting)											
	Main Heat Supply (W)	Heat Loss (W)		Total Loss**	Net Heat Through Sample (W)	Centerline Temperatures (°C)			Temperature Difference Across Sample (°C)	Final Results	
Run #	Q_{MH}	$QL_{back\ of\ heater}$	$QL_{lateral}$	%	Q_{STACK}	T_{MH}	R1CM	R2HM	ΔT	T_{MEAN} (°C)	k (W/(m K))
1*	31.11	4.23	3.62	25.23%	23.26	235.9	211.2	205.4	6.23	**208.2**	**4.90**
2*	63.4	8.69	7.25	25.14%	47.46	390.5	347.4	337.6	9.8	**342.5**	**6.36**
3	60.88	2.22	1.19	5.60%	57.47	529.5	493.2	483.1	10.03	**487.9**	**7.52**
4	96.11	2.39	2.18	4.75%	91.54	692.9	643.5	629.4	14.1	**636.5**	**8.53**
5	101.9	3.21	2.24	5.35%	96.44	736.5	684.5	670.3	14.47	**677.2**	**8.75**
6	116.6	3.13	4.86	6.85%	108.6	752.1	694.7	678.7	16	**686.7**	**8.91**
7	123	5.45	4.45	8.05%	113.1	779.9	720.1	703.6	16.5	**711.9**	**9.00**
8	121.62	3.48	5.08	7.04%	113.06	795.8	736.7	720.4	16.3	**728.6**	**9.11**
9	133.66	5.28	4.91	7.62%	123.47	851.7	786.4	769.5	17.07	**777.4**	**9.50**
10	140.74	7.15	5.91	9.28%	127.68	869	800.7	782.7	18	**791.7**	**9.32**
11	145.79	7.96	5.9	9.51%	131.93	888.3	820.7	802.1	19	**810.9**	**9.12**
12	150	7.93	6.03	9.31%	136.04	890.3	820.7	801.9	18.8	**811.3**	**9.50**
13	150	7.99	5.99	9.32%	136.02	895.4	826.5	807.4	19.1	**817.0**	**9.35**
14	147.86	6.6	4.3	7.37%	136.95	920.2	851	832	19	**840.8**	**9.47**
15	159.06	8.41	6.88	9.61%	143.78	925.1	852.3	831.9	20.77	**841.6**	**9.09**
16	149.2	5.16	4.12	6.22%	139.93	925.7	857.4	838.9	18.5	**848.2**	**9.93**
17	153.3	6.66	4.33	7.17%	142.3	940.8	871.3	852	19.67	**860.8**	**9.50**
18	158.78	6.79	5.3	7.61%	146.7	946.4	874.9	854.7	20.2	**864.8**	**9.54**

* guard heaters were off during these runs

** Total Loss = $(QL_{back\ of\ heater} + QL_{lateral})x100\%/Q_{MH}$

Table B.3: Heat Transfer Rate Calculation Comparison

Sample	Reference Plate 1				Reference Plate 2				Heat Transfer Comparison		
T_{MEAN} (°C)	T_{MEAN} (°C)	k_{ss} (W/mK)	ΔT (°C)	q_{R1} (W)	T_{MEAN} (°C)	k_{ss} (W/mK)	ΔT (°C)	q_{R2} (W)	Average of q_{R1} and q_{R2} (W)	q_{sample}* (W)	% Difference**
208.2	213.27	17.58	3.87	33.70	203.55	17.42	3.1	26.75	30.22	23.26	23.04%
342.5	350.7	19.68	6.6	64.33	334.3	19.46	6.6	63.61	63.97	47.46	25.81%
487.9	496.38	21.64	7.03	75.35	479.67	21.44	6.33	67.22	71.28	57.47	19.38%
636.5	648.1	23.62	9.2	107.63	624.8	23.3	9.2	106.17	106.90	91.54	14.37%
677.2	689.33	24.13	9.87	117.96	665.32	23.81	9.23	108.85	113.41	96.44	14.96%
686.7	699.7	24.26	10	120.16	673.7	23.94	10	118.57	119.37	108.6	9.02%
711.9	725.6	25.4	11	138.39	698.1	24.26	11	132.18	135.28	113.1	16.40%
728.6	742.35	25.4	11.3	142.16	714.9	24.33	11	132.56	137.36	113.06	17.69%
777.4	792.62	25.4	13.43	168.96	763.22	25.4	11.43	143.80	156.38	123.47	21.04%
791.7	807.2	25.4	13	163.55	776.35	25.4	12.7	159.77	161.66	127.68	21.02%
810.9	827.07	26.7	13.33	176.28	795.35	25.4	12.1	152.23	164.25	131.93	19.68%
811.3	827.2	26.7	13	171.92	795.55	25.4	12.7	159.77	165.85	136.04	17.97%
817.0	833	26.7	13	171.92	801.05	25.4	12.7	159.77	165.85	136.02	17.98%
840.8	857.38	26.7	14.1	186.47	825.28	26.7	12.37	163.59	175.03	136.95	21.75%
841.6	859.08	26.7	14.3	189.11	824.73	26.7	12.87	170.20	179.65	143.78	19.97%
848.2	864.2	26.7	13.6	179.85	831.95	26.7	13.9	183.82	181.84	139.93	23.05%
860.8	877.8	26.7	14.33	189.51	844.65	26.7	12.9	170.60	180.05	142.3	20.97%
864.8	881.83	26.7	13.87	183.42	847.7	26.7	14	185.14	184.28	146.7	20.39%

* q_{sample} is the heat transfer rate calculated by subtracting heat losses from heat supplied, as was used in the data reduction

** % Difference = $[(q_{R1} + q_{R2})/(2q_{sample}) - 1]x100\%$

Appendix C. Uncertainty Equations and Results

Uncertainty in Thermal Conductivity

$$k = \frac{q \cdot \Delta x}{A \cdot \Delta T} \tag{6}$$

$$\omega_k = \sqrt{\left(\frac{\partial k}{\partial \Delta x}\omega_{\Delta x}\right)^2 + \left(\frac{\partial k}{\partial A}\omega_A\right)^2 + \left(\frac{\partial k}{\partial \Delta T}\omega_{\Delta T}\right)^2 + \left(\frac{\partial k}{\partial q}\omega_q\right)^2} \tag{7}$$

$$\frac{\omega_k}{k} = \sqrt{\left(\frac{\omega_{\Delta x}}{\Delta x}\right)^2 + \left(\frac{\omega_A}{A}\right)^2 + \left(\frac{\omega_{\Delta T}}{\Delta T}\right)^2 + \left(\frac{\omega_q}{q}\right)^2} \tag{8}$$

Uncertainty in Area

$$A = w \cdot d \tag{9}$$

$$\frac{\omega_A}{A} = \sqrt{\left(\frac{\omega_w}{w}\right)^2 + \left(\frac{\omega_d}{d}\right)^2} \tag{10}$$

Uncertainty in Temperature Difference

$$\Delta T = T_2 - T_1 \tag{11}$$

$$\frac{\omega_{\Delta T}}{\Delta T} = \sqrt{\left(\frac{\omega_{T_2}}{\Delta T}\right)^2 + \left(\frac{\omega_{T_1}}{\Delta T}\right)^2} = \sqrt{2 * \left(\frac{\omega_T}{\Delta T}\right)^2} = \sqrt{2} * \frac{\omega_T}{\Delta T} \tag{12}$$

Uncertainty in Heat Transfer Rate

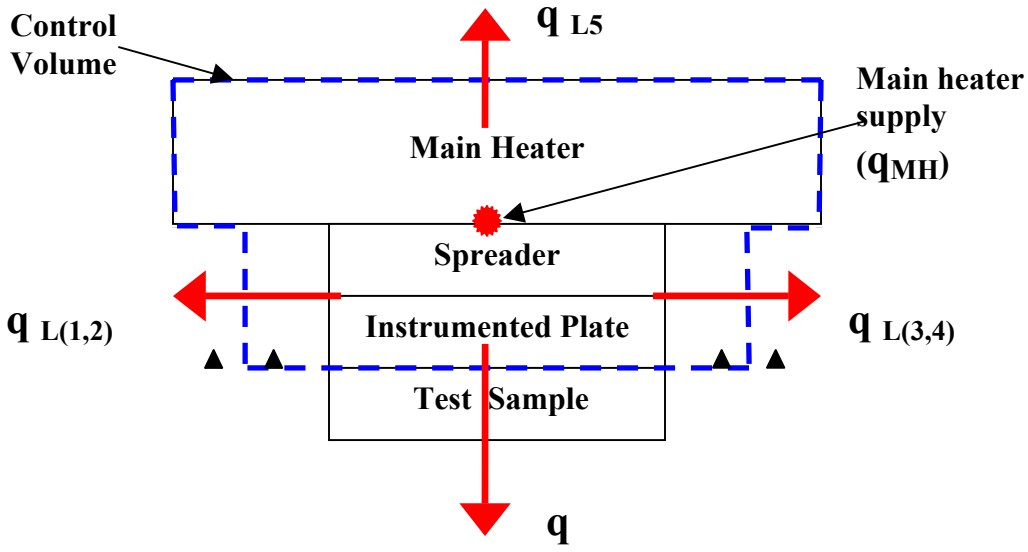

$$q = q_{MH} - q_{L1} - q_{L2} - q_{L3} - q_{L4} - q_{L5} \tag{13}$$

$$\frac{\omega_q}{q} = \sqrt{\left(\frac{\omega_{q_{MH}}}{q}\right)^2 + \left(\frac{\omega_{q_{L1}}}{q}\right)^2 + \left(\frac{\omega_{q_{L2}}}{q}\right)^2 + \left(\frac{\omega_{q_{L3}}}{q}\right)^2 + \left(\frac{\omega_{q_{L4}}}{q}\right)^2 + \left(\frac{\omega_{q_{L5}}}{q}\right)^2} \tag{14}$$

Uncertainty in Main Heater Power Supply

$$q_{MH} = V \cdot I \tag{15}$$

$$\frac{\omega_{q_{MH}}}{q_{MH}} = \sqrt{\left(\frac{\omega_V}{V}\right)^2 + \left(\frac{\omega_I}{I}\right)^2} \tag{16}$$

$$\frac{\omega_{q_{MH}}}{q} = \frac{\omega_{q_{MH}}}{q_{MH}} \cdot \frac{q_{MH}}{q} \tag{17}$$

Uncertainty in Heat Losses through Lateral surfaces and Back Surface of Main Heater (L1,2,3,4,5)

$$q_L = k_{ins} A_{eff} \frac{\Delta T_L}{\Delta x_{ins}} \tag{18}$$

$$\frac{\omega_{q_L}}{q_L} = \sqrt{\left(\frac{\omega_{k_{ins}}}{k_{ins}}\right)^2 + \left(\frac{\omega_{A_{eff}}}{A_{eff}}\right)^2 + \left(\frac{\omega_{\Delta T_L}}{\Delta T_L}\right)^2 + \left(\frac{\omega_{\Delta x_{ins}}}{\Delta x_{ins}}\right)^2} \tag{19}$$

$$\frac{\omega_{q_L}}{q} = \frac{\omega_{q_L}}{q_L} \cdot \frac{q_L}{q} \tag{20}$$

Uncertainty in Effective Area of Lateral Surfaces

$$A_{eff} = w_{eff} \cdot d_{eff} \tag{21}$$

$$\frac{\omega_{A_{eff}}}{A_{eff}} = \sqrt{\left(\frac{\omega_{w_{eff}}}{w_{eff}}\right)^2 + \left(\frac{\omega_{d_{eff}}}{d_{eff}}\right)^2} \tag{22}$$

The following uncertainties are assigned to measured values in calculating the final uncertainty of thermal conductivity of the sample.

$$\omega_{\Delta x} = \omega_w = \omega_d = .001"$$

$$\omega_{\Delta x_{ins}} = \omega_{w_{eff}} = \omega_{d_{eff}} = 1/64"$$

$$\omega_T = 0.3^{\circ} C$$

$$\omega_V = 0.5\% \ \textit{voltage reading}$$

$$\omega_I = 1\% \ \textit{current reading}$$

$$\omega_{k_{ins}} = 0.0037 \, W/mK$$

Table C.1: Uncertainty Results for the final results reported in Figure 6.1

Uncertainty Results								
Mean Temp	**ΔT**	**k**	**$\omega_{\Delta x}/\Delta x$**	**ω_A/A**	**$\omega_{\Delta T}/\Delta T$**	**ω_q/q**	**ω_k/k**	**ω_k**
°C	**°C**	**W/mK**						**W/(mK)**
208.220	6.230	4.903	0.0015	0.0003	0.068	0.020	0.071	**0.348**
342.500	9.800	6.360	0.0015	0.0003	0.043	0.019	0.047	**0.300**
487.850	10.030	7.525	0.0015	0.0003	0.042	0.012	0.044	**0.332**
636.450	14.100	8.526	0.0015	0.0003	0.030	0.012	0.032	**0.276**
677.170	14.470	8.753	0.0015	0.0003	0.029	0.012	0.032	**0.278**
686.700	16.000	8.914	0.0015	0.0003	0.027	0.012	0.029	**0.261**
711.850	16.500	9.002	0.0015	0.0003	0.026	0.012	0.029	**0.257**
728.550	16.300	9.109	0.0015	0.0003	0.026	0.012	0.029	**0.262**
777.370	17.070	9.499	0.0015	0.0003	0.025	0.012	0.028	**0.264**
848.150	18.500	9.933	0.0015	0.0003	0.023	0.012	0.026	**0.258**
840.833	19.000	9.466	0.0015	0.0003	0.022	0.012	0.026	**0.242**
791.700	18.000	9.315	0.0015	0.0003	0.024	0.013	0.027	**0.249**
811.300	18.800	9.503	0.0015	0.0003	0.023	0.013	0.026	**0.246**
816.950	19.100	9.352	0.0015	0.0003	0.022	0.013	0.026	**0.239**
810.900	19.000	9.119	0.0015	0.0003	0.022	0.013	0.026	**0.234**
841.550	20.770	9.091	0.0015	0.0003	0.020	0.013	0.024	**0.219**
860.800	19.670	9.501	0.0015	0.0003	0.022	0.012	0.025	**0.236**
864.800	20.200	9.537	0.0015	0.0003	0.021	0.012	0.024	**0.233**

Appendix D. Equipment and Material Lists

Equipment List

Computers

1. Hp 3456A Digital Voltmeter – UT# 368125
2. Hp 3497A Data Acquisition/Control Unit – UT# 368123
3. DELL Optiplex GX1 Computer (with HPVEE) – UT# 495158
4. DELL Precision 340 Computer (with Microsoft Excel) – UT# 495258
5. DELL Optiplex GX150 Computer (with internet access) – UT# 495243

Power Supply

6. Sorensen AC Regulator ACR 3000 – UT# 368118
7. Sorensen DC Power Supply – Model# DCR 300-9B2

Miscellaneous Electronics

8. Neslab Endocal RTE-110 Heating/Chilling, Recirculating Bath – Part# 163103200500
9. Corning Stirrer/Hot Plate – Model# PC-420
10. Cool-Arc Welder – UT# 283159
11. Fluke 117 True RMS Multimeter
12. Keithly Voltmeter Model 177 DMM

Heaters

13. Thermcraft Flat Plate Heater, 6”x10” – Model# FP-VFR-6-10
14. Thermcraft Flat Plate Heater, 8”x4” – Model# P-VFR-8-4

Thermocouples and Accessories

15. Miniature Thermocouple Connectors (Omega) – Model# HMPW-K-MF
16. Thermocouple Wire (K Type, Omega) – Model# GG-K-30-SLE-500
17. Nextel Braided Ceramic Very High Temperature Sleeving (Omega)
- Model# XC-116
18. Insulated Thermocouple Wire (Omega) – Model# EXTT-K-24-SLE
19. Tempco High-Temperature Lead Wire – Part# 2KE 36
20. Ceramic Connectors

Hand Tools

21. High Temperature Gloves
22. Storehouse Toolbox

Material List

Insulation

1. Kaowool Paper 700 Grade 1/8” Thick Insulation (Thermal Ceramics)
2. High Temperature 0.5” and 1” Thick Insulation Board (Thermcraft)
3. Ultra High-Temperature 1/16” Thick Millboard (McMaster)
4. Owens Corning R-19 Fiberglass Batting

Thermocouple Paste

5. Cermabond High-Temperature Adhesive (Aremco)

Stack Components

6. SiC Samples
7. Copper Plates
8. Aluminum Pieces
9. SS 304 Plates

Vita

Aaron Christopher Whaley was born in Knoxville, TN, on July 14, 1984. He grew up in Farragut, TN. Aaron graduated from Farragut High School in 2002. He went on to the University of Tennessee, Knoxville, and received a B.S. in Mechanical Engineering in 2006. Aaron is currently completing a M.S. in Mechanical Engineering, also at the University of Tennessee, Knoxville.